

# Calibration of the MEMS v1 model over a continental soil inventory: a comparison of MCMC and 4DEnVar methods ~~Comparing the MEMS v1 model performance with MCMC and 4DEnVar calibration methods over a continental soil inventory~~

Toni Viskari<sup>1</sup>, Tristan Quaife<sup>2</sup>, Fernando Fahl<sup>1</sup>, Yao Zhang<sup>3</sup>, and Emanuele Lugato<sup>1</sup>

<sup>1</sup> European Commission, Joint Research Centre (JRC), Ispra, Italy

<sup>2</sup> National Centre for Earth Observation, Department of Meteorology, University of Reading, United Kingdom

<sup>3</sup> Natural Resource Ecology Lab, Colorado State University, USA

Correspondence to: Toni Viskari (toni.viskari@ec.europa.eu)

**Abstract.** An abundant amount of different data is required to calibrate soil organic carbon (SOC) models to represent ecosystems at large-scale. However, due to challenges related to model state projections, this calibration becomes very computationally heavy with traditional calibration methods. ~~In this work, w~~Here, we test 4-Dimensional Ensemble Variational data assimilation (4DEnVar) method to parameterize the MEMS v1 SOC model using data from the LUCAS ~~soil sampling~~ network and compare its performance against MCMC calibration. Additionally, we performed an experiment where we adjusted the litter input calculation to see if the two calibration methods react differently to the change. Comparing ~~the~~ The total SOC projections from both parameterizations ~~and validation datasets~~ showed similar improvements ~~even~~ though the produced parameter sets differed. A thorough analysis revealed that the detailed SOC states ~~were not similar to a meaningful degree~~ differed from each other, but we also lacked information to determine which parameter set was closer to the truth. Furthermore, changing the litter input partition highlighted how much that assumption affects the calibration results with both methods. Our results here establish 4DEnVar as an applicable calibration method for SOC models but also highlight the need for more nuanced validation methods, as well as careful examination on how different data sets affect the model calibration.

## 1 Introduction

Soil organic carbon (SOC) stocks are a major component of the global carbon cycle (Scharlemann et al., 2014) and are inherently linked to surface vegetation, as the long-term SOC compounds forming them are produced by decomposition of plant litter (Cornwell *et al.*, 2008). Due to the importance of those stocks, they are a central part of national carbon budgets (van den Berg et al., 2020) and targeted by climate related policy (e.g. LULUCF, CRCF; Schlamadinger et al., 2007) aiming at enhancing carbon accumulation into the soils and improve terrestrial carbon sinks (Rumpel et al., 2020). All of this has also highlighted the need to improve the current soil related Monitoring, Reporting and Verification (MRV) systems (Bellassen *et al.*, 2015).

Soil inventory and numerous measurement campaigns, both temporary and continuous, have been set up to actively observe the soil carbon states within given regions and/or ecosystems (Smith et al., 2020). While these provide valuable information about the SOC stocks in that time window, also utilizing faster sample collections and analysis (Loria *et al.*, 2024), they generally provide only information on the total SOC stocks.

~~Indeed, current understanding of SOC cycling has been recently advanced s~~To provide more nuanced SOC measurements, separating the bulk soil into SOC fractions (Cambardella and Elliot, 1992; Lavallee et al., 2019; Yu et al., 2022), notably the mineral-associated (MAOM) and the particulate organic matter carbon (POM), has been utilized more in current field campaigns. However, F though there are different methods to measure these short- and long-lived SOC fractions (Delahaie et al., 2024), they require considerable resources to be applicable

44 on a large spatial scale. Thus, models are a crucial tool in both providing more cost-effective estimates of SOC  
45 states across landscapes, as well as their responses to both climate and environmental changes.

46 To this purpose, numerous models of varying complexities have been developed (Chandel et al., 2023; Le Noë  
47 et al., 2023) with different approaches and focuses. -have been developed from Some are simple first-order  
48 dynamic models such as RothC (Coleman and Jenkins, 1996) ~~to~~ while others are more complicated non-linear  
49 models such as MIMICS (Wieder et al., 2014) and Millennial (Abramoff et al., 2022). However, the lack of  
50 detailed information both regarding the SOC state and drivers, such as litter and soil moisture, does affect the  
51 ability to reliably constrain the various processes included into the models. Therefore, it is necessary to calibrate  
52 the model with more measurements from different pedo-climatic and land cover conditions, in order to capture  
53 how they affect the SOC state. This, though, increases the computational cost of the calibration.

54 Additionally complicating matters is ~~that~~ even when using spatially diverse data for calibration, there are  
55 numerous assumptions regarding how that driver data is applied within the model that will affect not just model  
56 forward projections, but also the calibration process itself. For example, NPP is commonly used as a proxy for  
57 litterfall in SOC models (e.g. Abramoff et al., 2022; Pierson et al., 2022), with empirical work showing that the  
58 approach is justified (Matthews, 1997). How this NPP should be divided between above- and belowground  
59 biomass and, consequently between different model pools, depends on the ecosystem (Jevon et al., 2022; Cao et  
60 al., 2024) and is critical for determining the soil litter input. Without much more detailed information than is  
61 often available, these NPP/litter related parameter cannot be simultaneously calibrated with the SOC model  
62 parameters because of how fundamentally those values are connected; increasing/decreasing the amount of soil  
63 litter will simply result in an increase/decrease in decomposition rates to fit the measured SOC values. While  
64 there are valuable additional measurement datasets such as 14C (Brunmayer et al., 2024) that can provide  
65 important additional constraints for determining effective litter inputs, even these are still affected by how the  
66 NPP input is presented to start with in the model. This is just one example of driver associated assumptions and  
67 a quick nimble calibration method is needed to assess how these uncertainties impact the calibration results.

68 The traditional grand standard for model calibration is the Monte Carlo Markov Chain Metropolis Hastings  
69 algorithm (MCMC; Geyer, 1992). This is a very computationally heavy approach with multiple variants having  
70 been developed over the years to make it more efficient in exploring the parameter space and avoid local  
71 likelihood maximas in its search for the most likely parameter sets (e.g Papaioannou et al., 2015; Vrugt, 2016).  
72 Due to the challenges discussed before, only computationally light SOC models can be calibrated within a  
73 practical time frame using large scale data (for example Tuomi et al., 2009). There have been workarounds  
74 presented, making assumptions about the initial state (Nemo, 2017; Mathers et al., 2023), using simpler  
75 calibration methods (Gurung et al, 2020) or taking advantage of machine learning approaches (Heuvelink et al.,  
76 2021). However, there remains a need for a fast and trustworthy calibration method for SOC models that would  
77 allow for easy experimentation on how different datasets affect the calibration or constraining new model  
78 dynamics being included. For example, equifinality is a known issue in ecosystem modelling, where there are  
79 multiple parameter sets that produce a similar model output (Sierra et al., 2015; Marschmann et al., 2019).  
80 Establishing if this is affecting the model system under study requires repeating the calibration multiple times  
81 which is prohibited by too heavy calibration approaches.

82 As a more practical alternative to the costly MCMC approach, four-dimensional ensemble variational data  
83 assimilation (4DEnVar; Liu et al., 2008) is a novel data assimilation approach, where a model ensemble  
84 generated by varying the parameters/variable states of interest is used to determine the optimal parameter and/or  
85 state variables. It has already been used for parameter calibration (Douglas et al., 2025; Pinnington et al. 2020)  
86 and is much faster than the traditional MCMC methods. Similarly to MCMC, in It is based on the Four-  
87 dimensional Variational data assimilation (4DVar; Le Dimet and Talagrand, 1986), where a model projection is  
88 compared with observations and the new initial state for the next iteration is generated from this information. A  
89 key difference between MCMC and 4DVar based methods is that the latter uses gradient descent methods to  
90 determine the next state instead of randomly sampling. While ~~this method~~ 4DVar has initially been used more  
91 commonly for state data assimilation, for example, in weather forecast (Huang et al., 2009), it has also been  
92 successfully applied to calibrate ecosystem models (e.g. Raoult et al., 2016; Peylin et al., 2016; Pinnington et al.  
93 2016). However, to implement 4Dvar with observations from multiple different times, an adjoint version of the  
94 model is needed which imposes its own challenges and limitations on the application (Thepaut and Courtier,  
95 1991). The 4DEnVar method uses the ensemble to sidestep this requirement by simultaneously running multiple  
96 simulations with different parameter sets instead of an iterative solution. While to our knowledge there haven't

97 been previous studies within the ecosystem modelling analysing the performance of the 4DEnVar to that of  
98 MCMC, in Beylat et al. (2025) the 4DEnVar method is compared to the original 4DVAR method in a very  
99 specific synthetic experiment. Within that scope the 4DEnVar was shown to be more effective than the original  
100 version, but it is only the first step in evaluation. Four dimensional ensemble variational data assimilation  
101 (4DEnVar; Liu et al., 2008) is a novel data assimilation approach, where an ensemble is used to sidestep the  
102 need for the model adjoint. It has already been used for parameter calibration (Douglas et al., 2025; Pinnington  
103 et al. 2020) and is much faster than the traditional MCMC methods as it requires far fewer model iterations.

104 In the work presented here, we calibrated the MEMS v1 SOC model (Robertson et al., 2019) with both MCMC  
105 and 4DEnVar parameterization methods. The model in question simulates organic carbon decomposition  
106 separately for above- and below-ground carbon with pathways from surface vegetation matter to the soil pools.  
107 In the framework of the MEMS v1, the microbial pool is the central connection between the different SOC  
108 states and, crucially, along with the soil properties regulates the amount of carbon stored as long-lived MAOM  
109 compounds. The SOC pools are for the most part connected by first order dynamics, but the relationship  
110 between the microbial and MAOM pool is non-linear. Consequently, there is only a small number of central  
111 parameters to calibrate while simultaneously the model steady state cannot be analytically solved, requiring the  
112 more costly parameterization process.

113 Soil data from the Land Use/Land Cover Area Frame Survey (LUCAS) measurement network (Orgiazzi et al.,  
114 2018) were used for calibration and validation against estimated model parameters, assessing their performances  
115 relative to each other and the default parameters. Because this LUCAS dataset contains measurements from  
116 thousands of plots across Europe and, thus, represents many different types of ecosystems as well as climate  
117 conditions, it allows to test a wider performance of the model calibration. One of the advantages was the level of  
118 standardisation in sample collection and analysis, the latter done by a unique laboratory. Furthermore, for a  
119 small subset of the chosen LUCAS dataset, the POM/MAOM fractioning also had been done, which provided  
120 more nuanced information for the calibration process. While Lucas is a standardised framework for SOC, was  
121 not specifically designed to assess the MAOM stocks.

122 Our hypothesis is that the 4DEnVar improves the model fit to a sufficient degree~~the same degree~~ that, along  
123 with the reduced computational cost, it can be considered as valid calibration approach for SOC models as the  
124 MCMC, ~~with much less computational cost~~. Specifically, there are two objectives for the work presented here:  
125 the first is to test if the much faster 4DEnVar calibration performs as well as the MCMC calibration and  
126 examine if there are any meaningful differences in the resulting parameter sets; the second is to conduct a  
127 simple experiment where we made a change on how the NPP litter input was ~~partitioned~~ deallocated. The  
128 reasoning for the latter objective is that one of the core benefits of the faster calibration method is that it allows  
129 testing how different assumptions impact the parameterizations. Because of this, if there are differences between  
130 the results of the two calibration methods, it is important to assess if the general behaviour of the  
131 parameterizations remains the same even under different assumptions. The intent here is to see both how this  
132 will affect the calibration and if the two methods respond similarly to the change.

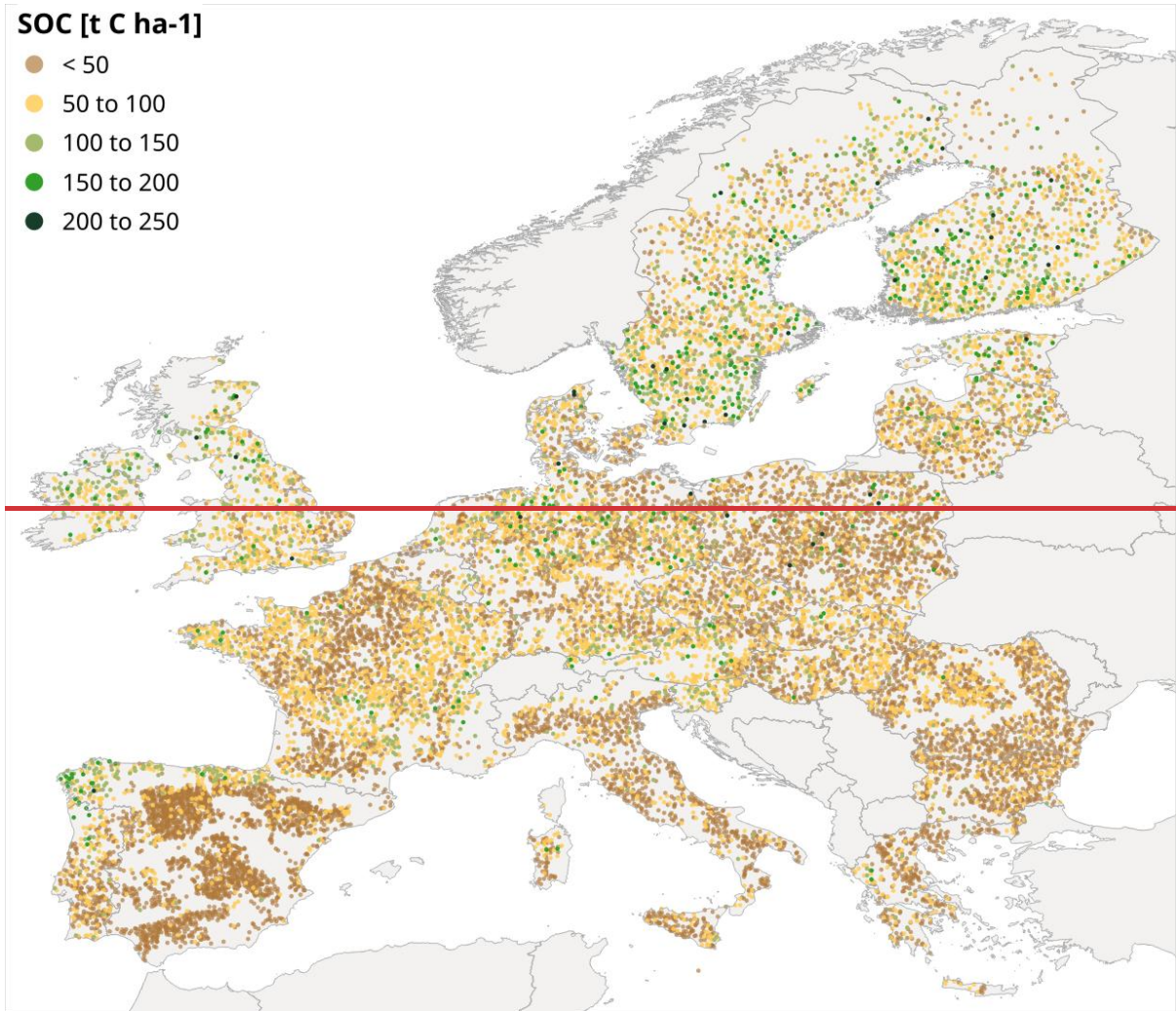
## 134 2. Methods and data

### 135 2.1 LUCAS measurements

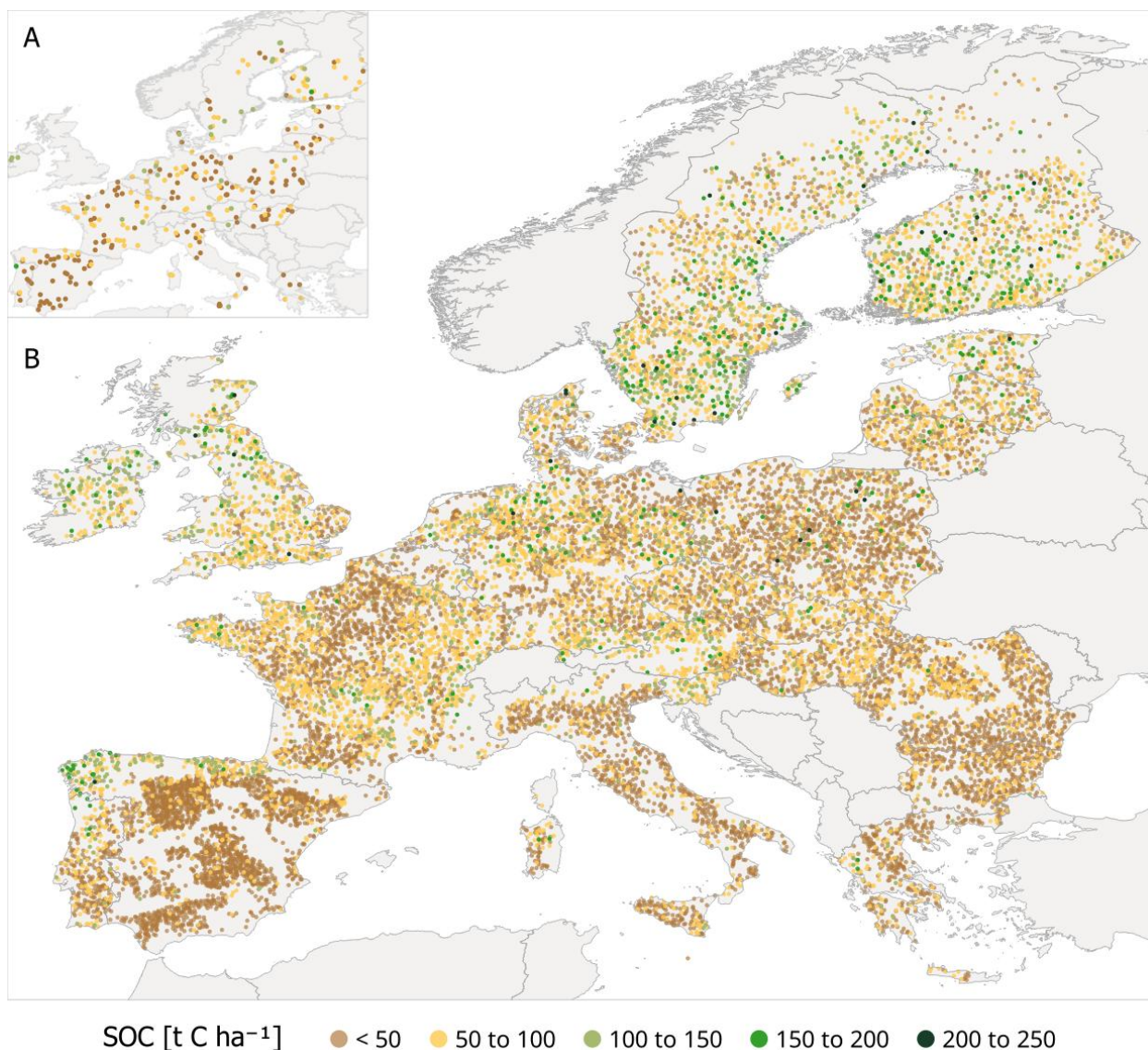
136 For the ~~MEMS~~ model calibration, we used the LUCAS points from a field campaign conducted in 2009 as  
137 reported in (Cotrufo et al., 2019 and; Lugato et al., 2021). This dataset comprises; 1) the main physico-chemical  
138 characteristic of topsoil (0-20 cm), including total SOC content for about 20.000 samples distributed across  
139 different land covers in the EU and UK; 2) a size-fraction of the bulk SOC into mineral-associated (MAOM)  
140 and particulate organic matter carbon (POM) in a representative sub-set of 350 samples. The latter were  
141 randomly drawn from the all the measurements with the only constraint being that both datasets were similarly  
142 distributed across ecosystems with ~~Both the calibration and total dataset are similarly distributed across~~  
143 ~~ecosystems with~~ approximately 73 % being grass- or croplands with the rest being various forest types. Figure 1  
144 shows the LUCAS data points across Europe and the calculated SOC stock at each measurement site. The  
145 representativeness of the chosen 350 measurements points is elaborated upon in Lugato et al. (2021).

**SOC [t C ha<sup>-1</sup>]**

- < 50
- 50 to 100
- 100 to 150
- 150 to 200
- 200 to 250



146



147

148 **Figure 1: The LUCAS 2009 sampling points across Europe and their SOC stock used for A) calibration and B)**  
 149 **validation.**

150 For the calibration, the 348 LUCAS measurements from the 2009 campaign containing POM/MAOM fractions  
 151 are used. The remaining 19 476 total SOC measurements were set aside for validation. In both allocations,  
 152 measurements which were not classified as agricultural, grassland or forest were removed as well as all the  
 153 sampling points where the driver data was not available. As a result, 322 datapoints are used for calibration and  
 154 17 430 for validation.

155 While the benefit of the LUCAS dataset is its large spatial representation and inclusion of measurements from  
 156 multiple different ecosystems, the execution of such a vast measurement campaign introduces different source  
 157 of errors from sampling, labelling, analysis etc. Thus, it is almost more apt to be considered as a combination of  
 158 several independent campaigns done with the same protocols, instead of a single consistently controlled  
 159 campaign. Additionally, although locations of the measurement are known, we have to make the assumptions  
 160 that the available driver data are representative for the actual conditions at the measurement plot.

161

162 **2.2 MEMS mode and /pParameters chosen for calibration**

163 The Microbial Efficiency-Matrix Stabilization V1 (referred to simply as MEMS for simplicity; Robertson et al.,  
 164 2019) model is a novel soil organic carbon (SOC) model framework, which is built around the scientific

165 understanding that the soil microbial pool modulates the SOC stocks. The model structure is presented in  
 166 Supplemental Figure 1. In the model, both surface vegetation and SOC decomposition are represented by  
 167 multiple pools defined by their physical properties. There are several paths for carbon fluxes to transfer from  
 168 one pool to another or lost as CO<sub>2</sub>, with the rate of change calculated on a daily timestep. The model dynamics  
 169 represents the depth of the soil measurements used to calibrate it. As we are using the LUCAS data here which  
 170 is from the top 20 cm of the soil, the resulting MEMS model will thus simulate the SOC dynamics of top 20 cm  
 171 layer as well.

172 Since the calibration parameterization, here, focuses on the SOC stock, only the model equations affecting  
 173 MEMS pools C5 (Heavy particulate organic matter), C8 (Dissolved organic matter), C9 (Mineral associated  
 174 organic matter (MAOM)) and C10 (Light particulate organic matter) were calibrated here considered in this work.  
 175 While the surface-vegetation decomposition pools C1 (hot-water soluble), C2 (acid soluble) and C3 (acid  
 176 insoluble) as well as the surface microbial pool (C4) and the dissolved organic matter (C6) do determine the  
 177 litter input entering to soil C pools, these mechanics were not included in the calibration as the type of data  
 178 required to constrain them was not available. Therefore, we used the default parameters values established in  
 179 Robertson et al. (2019) for the surface processes since they had been chosen to be representative of the LUCAS  
 180 network environment. Meanwhile the released CO<sub>2</sub> (C7) and the leached dissolved material to the soil (C11) are  
 181 cumulative removal pools and do not have any parameters to be calibrated.

182 The equations that govern the change in the relevant pools in MEMS are:

$$183 \frac{dC_5}{dt} = C_{5,in}^2 + C_{5,in}^3 + C_{5,in}^4 - T_{mod}k_5C_5 \quad (1)$$

$$184 \frac{dC_8}{dt} = C_{8,in}^5 + C_{8,in}^6 + C_{8,in}^{10} - sorp - DOC_{lch}C_8 - T_{mod}k_8C_8 \quad (2)$$

$$185 \frac{dC_9}{dt} = sorp - T_{mod}k_9C_9 \quad (3)$$

$$186 \frac{dC_{10}}{dt} = C_{10,in}^2 + C_{10,in}^3 - T_{mod}k_{10}C_{10} \quad (4)$$

187 Where  $C_i$  is the amount of carbon stored in pool  $i$ ,  $C_{i,in}^j$  is the carbon input to pool  $i$  from pool  $j$  as a result of the  
 188 decomposition process and  $k_i$  is the decomposition rate for pool  $i$ . The leaching coefficient  $DOC_{lch}$  represents  
 189 the dissolution of SOC to deeper soil layers and the temperature coefficient  $T_{mod}$  reflects how soil temperature  
 190 affects the decomposition rate. In this work,  $T_{mod}$  is the same for all pools and follows the STANDCARB 2.0  
 191 model (Harmon et al., 2009) which is an expanded version of the traditional Q10 temperature model where the  
 192 limiting impact of the high temperatures is accounted for.

193 The sorption coefficient  $sorp$  controls the flow of carbon between the microbial pool and the mineral associated  
 194 carbon pool as determined by the equation

$$195 sorp = C_8 \frac{K_{lm}Q_{max}C_8 - C_9}{1 + K_{lm}C_8} \quad (5)$$

$$196 Q_{max} = d \cdot \rho_{soil} \cdot (1 - p_{rock}) \cdot sc_{conc} \quad (6)$$

$$197 sc_{conc} = sc_{slope} \cdot (1 - p_{sand}) + sc_{int} \quad (7)$$

198 In which  $K_{lm}$  is the langmuir isotherm term that depends on the soil pH,  $Q_{max}$  is the maximum absorption  
 199 capacity of the soil,  $\rho_{soil}$  is the soil bulk density,  $p_{rock}$  is the rock percentage of the soil and  $p_{sand}$  is the sand  
 200 percentage of the soil. The maximum concentration of fine fraction,  $sc_{conc}$ , is governed by the two coefficients  
 201  $sc_{int}$  and  $sc_{slope}$ . Consequently, those two parameters effectively control the saturation ratio for the MAOM  
 202 pool.

203 The decomposition rate parameters  $k_5$ ,  $k_8$ ,  $k_9$  and  $k_{10}$  were the central parameters chosen for calibration as well  
 204 as  $sc_{int}$  and  $sc_{slope}$ . As the primary focus of this work is to compare the calibration methods, these parameters  
 205 were simply chosen as a straight-forward test case. The boundary values are presented in Table 1. As will  
 206 explained in Section 2.5, we do need an expected value for these parameters in order to create a prior  
 207 uncertainty distribution. As prior values for our calibration, we chose this value also set randomly drawn and

208 ~~rounded values for~~ by randomly drawing a parameter value from the parameters near the middle of the set of the  
 209 boundary conditions after testing that the model runs remained stable with these parameter values.

Name	Symbol	<u>Expected value</u> <del>Prior</del>	Minimum value	Maximum value
Decomposition rate for <u>heavy particle organic matter</u> Pool (C5; day <sup>-1</sup> )	k <sub>5</sub>	0.0008	0.0001	0.002
Decomposition rate for <u>dissolved soil organic material</u> pool (C8; day <sup>-1</sup> )	k <sub>8</sub>	0.001	0.0001	0.01
Decomposition rate for <u>mineral associated matter</u> pool (C9; day <sup>-1</sup> )	k <sub>9</sub>	0.000025	0.00001	0.00004
Decomposition rate for <u>light particle organic matter</u> pool (C10; day <sup>-1</sup> )	k <sub>10</sub>	0.0005	0.0001	0.0004
Saturation intercept	SC <sub>Intercept</sub>	10.0	5	20
Saturation slope	SC <sub>Slope</sub>	0.25	0.1	0.4

210

211 **Table 1: The calibrated parameters chosen for calibration, their assigned expected baseline-parameter values as well**  
 212 **as boundaries that constrain the lowest and highest values that the parameters are allowed be given during the**  
 213 **calibration.**

214

215 To determine how we divide the litter input to MEMS model pools, the site ecosystem type was assigned by the  
 216 Corine Land Cover (Buttner, 2014). Following that, NPP is split into the MEMS model pools according to the  
 217 following framework established in Robertson et al. (2019):

$$218 \quad C_{1,input}(t) = (1 - f_{doc}^{eco})f_{sol}^{eco}r^{eco}NPP(t) \quad (8)$$

$$219 \quad C_{2,input}(t) = (1 - f_{sol}^{eco} - f_{lig}^{eco})r^{eco}NPP(t) \quad (9)$$

$$220 \quad C_{3,input}(t) = f_{lig}^{eco}r^{eco}NPP(t) \quad (10)$$

$$221 \quad C_{6,input}(t) = f_{sol}^{eco}f_{doc}^{eco}r^{eco}NPP(t) \quad (11)$$

222 Where  $C_{i,input}(t)$  is the carbon input to pool  $i$  from  $NPP$  at a given time  $t$  and  $eco$  refers to the ecosystem for the  
 223 LUCAS point. Then,  $f_{sol}$  is the hot water extractable fraction of the litter input,  $f_{doc}$  is the cold-water  
 224 extractable fraction of the water extractable fraction and  $f_{lig}$  is the acid-insoluble fraction of the of the litter  
 225 input. It is important to note that these fractions are not the totality of the litter input and, while equations from  
 226 ~~847~~ to ~~1120~~ do sum up to the total  $NPP$ , the fractions presented here do not sum up to 1. Finally, the  $r^{eco}$   
 227 represents the fraction of  $NPP$  that is assumed to have been removed from the system due to economic activities  
 228 (harvest, grazing, etc.)

229 The coefficient values based on Campbell et al. (2016) are presented in Table 2. It is important to make two  
 230 notes regarding these values. First, we are using a single fraction here and do not account for the uncertainty  
 231 range provided in the work referenced. Second, only  $f_{sol}$  and  $f_{lig}$  fraction ranges are presented in Campbell et  
 232 al., (2016). For  $f_{doc}$  we used a constant value across land covers in line with the work Robertson et al. (2019).

	NPP fraction ( $r^{eco}$ )	<u>Hot water</u> <u>extricable fraction</u> ( $f_{sol}$ )	<u>Acid insoluble</u> <u>fraction</u> ( $f_{lig}$ )	<u>Cold water</u> <u>extricable fraction</u> ( $f_{doc}$ )
Woody grassland	0.67	0.35	0.15	0.15
Pure grass	0.51	0.35	0.15	0.15

Sporadic grassland	0.59	0.35	0.15	0.15
Cropland	0.43	0.35	0.15	0.15
Mixture	0.77	0.375	0.295	0.15
Broadleaf	0.68	0.4	0.27	0.15
Conifer	0.78	0.35	0.32	0.15

233

234 **Table 2: The fraction of NPP that is used for litter input and how it is divided into different litter**  
235 **compounds**

236

237

### 238 2.3 MCMC

239 Markov Chain Monte Carlo (MCMC; Geyer, 1992) is a widely used Bayesian model parameterization method.  
240 The basis of this approach is straightforward: First values for the parameters chosen for calibration are drawn by  
241 randomly perturbing accepted parameter values and the model is run for given locations with these parameters.  
242 Assuming that the uncertainties are normally distributed, the total likelihood  $F$  of these projections, given  
243 observations that correspond to model predictions, is calculated with

$$244 F = \prod_{l=1}^{N_{obs}} (2\pi\sigma_l^2)^{-\frac{1}{2}} e^{-\frac{1}{2}\sum_{l=1}^{N_{obs}} \frac{(x_l - y_l)^2}{\sigma_l^2}} \cdot \prod_{k=1}^{N_{par}} (2\pi\sigma_{\theta,k}^2)^{-\frac{1}{2}} e^{-\frac{1}{2}\sum_{l=1}^{N_{par}} \frac{(\theta_k - \theta_{k,prior})^2}{\sigma_{\theta,k}^2}} \quad (12)$$

245 Where  $l$  is the observation index,  $N_{obs}$  is the number of observations,  $\sigma$  is the associated uncertainty,  $x_l$  is the  
246 model projection with parameter set  $\theta$  and  $y_l$  is the observation for index  $l$ . Furthermore,  $k$  is the parameter  
247 index,  $N_{par}$  is the number of parameters being estimated and  $\theta_{prior}$  is the prior estimate of parameters.

248 Once the likelihood is determined, it is compared to the likelihood of the previously accepted parameter set. If  
249 the new likelihood is higher, then that parameter set is automatically accepted and used as the parameters for the  
250 next iteration. However, if the new likelihood is lower than the previous one, there is still a probability that the  
251 new parameter set will still be accepted depending on how close the new likelihood is to the previous accepted  
252 likelihood.

253 By allowing the lower likelihoods to be possibly accepted, MCMC also provides an acceptable parameter range,  
254 which can be used to represent the parameter uncertainties. This iterative process is repeated until a given  
255 convergence goal is satisfied (Roy, 2020).

256 For the study here, we used the MCMC framework established in Viskari et al. (2022), which utilizes the  
257 BayesianTools R-library (Hartig et al., 2019). The chosen MCMC algorithm is the Differential evolution  
258 Markov Chain with snooker updater (DEzs; ter Braak and Vrugt, 2008), where multiple calibration chains  
259 progress concurrently from different starting point with information shared between the chains at given  
260 intervals. This should lead to a more efficient and faster convergence of the calibration, especially as this  
261 approach makes it possible to parallelize the different chains.

262 Six chains were used for the calibration with the initial values for each chain randomly drawn from the prior  
263 parameter range. The MCMC was run for 100 000 accepted iterations with the convergence test and statistical  
264 values calculated from the last 10 000 iterations.

265

### 266 2.4 4-Dimensional Ensemble Variational assimilation

267 Instead of iteratively exploring the variable space like MCMC does, 4-Dimensional Ensemble Variational data  
268 assimilation (4DEnVar) uses an ensemble of model runs with different variable sets and that are independent of  
269 each other. The ensemble of model runs is used to approximate information required by other calibration  
270 techniques, such as the gradient of the cost function and a mapping from variable space to observation space.  
271 Because there is no need for a large amount of model run repetitions such as in MCMC, this method is a  
272 computationally much faster. However, this approach is built on certain assumptions – in particular that the

273 observations can be predicted by a linear combination of the different ensemble members - which make it  
 274 important to test before-hand how well it is able to find the correct values in different systems.

275 The foundational theory for ~~4-Dimensional Ensemble Variational data assimilation (the 4DVar)~~ 4DEnVar method is  
 276 explained in Liu *et al.* (2008). The formulation established in Pinnington *et al.* (2020) was used as the basis for  
 277 this work. In this section, we will provide a simplified description of the method as it applies to our purposes.

278 In traditional baseline 4-Dimensional Variational data assimilation (4DVar; Le Dimet and Talagrand, 1986),  
 279 similarly to MCMC, the most likely state, i.e. the model parameter set, is solved by determining the minimum of  
 280 the cost function  $J$

$$281 \quad J = \frac{1}{2} ((\boldsymbol{\theta} - \boldsymbol{\theta}_{prior})^T \mathbf{B}^{-1} (\boldsymbol{\theta} - \boldsymbol{\theta}_{prior}) + \sum_{t=1}^K (M_{0 \rightarrow t}(\boldsymbol{\theta}, \mathbf{x}_0) - \mathbf{y}_k)^T \mathbf{R}_t^{-1} (M_{0 \rightarrow t}(\boldsymbol{\theta}, \mathbf{x}_0) - \mathbf{y}_k)) \quad (13)$$

282 In which  $\boldsymbol{\theta}$  and  $\boldsymbol{\theta}_{prior}$  are, respectively, the suggested and prior parameter value vectors,  $\mathbf{B}$  is the prior  
 283 parameter error covariance matrix and  $\mathbf{R}_t$  is the observation error covariance matrix at the measurement time  $t$ .  
 284 The model operator  $M_{0 \rightarrow t}$  calculates from the given parameters and the initial state  $\mathbf{x}_0$  the output comparable to  
 285 the observation vector  $\mathbf{y}_k$ . The measurement times in the chosen time window is represented by  $K$ .

286 Two brief notes on this formulation. First, it is essentially the same as exponent component in Eq 128, except  
 287 that is written it in vector form. Second, in an effort to simplify the equations, we did not include  
 288 ~~an observation an~~ an observation operator component in the equations. All our observations are point measurements  
 289 that can be directly compared with the model output, hence a separate observation operator was unnecessary for  
 290 our purposes.

291 4DVar, like MCMC, is also an iterative approach that calculates the cost function with different state vectors to  
 292 test if the cost function value decreases. However, with 4DVar, the iterations suggested after the first attempt are  
 293 not randomly drawn, but rather determined by the gradient function

$$294 \quad \nabla J = \mathbf{B}^{-1} (\boldsymbol{\theta} - \boldsymbol{\theta}_{prior}) + \sum_{t=1}^K \mathbf{M}_{0 \rightarrow t}^T \mathbf{R}_t^{-1} (M_{0 \rightarrow t}(\boldsymbol{\theta}, \mathbf{x}_0) - \mathbf{y}_k) \quad (14)$$

295 Where  $\mathbf{M}_{0 \rightarrow t}^T$  is the adjoint of the tangent-linear version  $\mathbf{M}_{0 \rightarrow t}$  of the model operator  $M$ .

296 The benefit of the gradient use is that it results in a value of zero for the state vector that produces the cost  
 297 function minimum. Thus, gradient descent techniques (Ruder, 2016) are able to use the information from the  
 298 gradient to efficiently locate the cost function minimum and the optimal state vector.

299 Naturally, there are challenges in applying this method. The core hurdle is the adjoint operator in equation Eq.  
 300 140, which is the transpose of the tangent-linear version of process model. Creating these model versions,  
 301 though, is not a simple task and imposes a linearity assumption on the driving processes. Furthermore, since  
 302 background error covariance matrix  $\mathbf{B}$  can have non-diagonal terms representing error covariances, the inverse  
 303 matrix can become computationally implausible to be calculated for larger systems.

304 In 4DEnVar, these issues are approached by expanding on the square root transform framework established in  
 305 Tippett *et al.*, 2003. Let us have an ensemble of model runs where, in our case, every ensemble has a different  
 306 parameter set randomly drawn from the same baseline prior distribution. In the 4DEnVar formulation, this prior  
 307 distribution is assumed normally distributed. For each ensemble member, we can then determine how its output  
 308 differs from the prior parameter set output. These perturbations from the mean across the ensemble can be  
 309 written in matrix format  $\boldsymbol{\Theta}'_b$  as follows

$$310 \quad \boldsymbol{\Theta}'_b = \frac{(\boldsymbol{\theta}^{b,1} - \bar{\boldsymbol{\theta}}^b, \boldsymbol{\theta}^{b,2} - \bar{\boldsymbol{\theta}}^b, \boldsymbol{\theta}^{b,3} - \bar{\boldsymbol{\theta}}^b, \dots, \boldsymbol{\theta}^{b,L} - \bar{\boldsymbol{\theta}}^b)}{\sqrt{L-1}} \quad (15)$$

311 Where  $L$  is the ensemble size,  $\boldsymbol{\theta}^{b,i}$  is the  $i$ th vector of the perturbation matrix, and  $\bar{\boldsymbol{\theta}}^b$  is the average over the  
 312 perturbations. In our case, the average over the perturbations is the same as the prior parameter vector  $\boldsymbol{\theta}_{prior}$ .

313 Since this matrix essentially represents the uncertainty related to the parameter values, the prior error covariance  
 314 matrix  $\mathbf{B}$  can be approximated as

$$315 \quad \mathbf{B} \approx \boldsymbol{\Theta}'_b \boldsymbol{\Theta}'_b{}^T \quad (16)$$

316 We admit that in this formulation we ignore model structural error and assume the dominant error is from the  
 317 parameter uncertainty.

318 Furthermore, we can define a vector  $\mathbf{w}$  with the length of  $L$  that satisfies the equation

$$319 \quad \mathbf{w} = \boldsymbol{\Theta}'_b^{-1}(\boldsymbol{\theta} - \boldsymbol{\theta}_{\text{prior}}) \quad (17)$$

320 With these formulations and assumptions, the cost and gradient functions can be written as

$$321 \quad \mathbf{J}(\mathbf{w}) = \frac{1}{2} \mathbf{w} \cdot \mathbf{w}^T + \frac{1}{2} \sum_{t=1}^K (\mathbf{M}_{0 \rightarrow t} \boldsymbol{\Theta}'_b \mathbf{w} + M_{0 \rightarrow t}(\boldsymbol{\theta}, \mathbf{x}_0) - \mathbf{y}_k)^T \mathbf{R}_t^{-1} (\mathbf{M}_{0 \rightarrow t} \boldsymbol{\Theta}'_b \mathbf{w} + M_{0 \rightarrow t}(\boldsymbol{\theta}, \mathbf{x}_0) - \mathbf{y}_k) \quad (18)$$

$$322 \quad \nabla \mathbf{J}(\mathbf{w}) = \mathbf{w} + \sum_{t=1}^K \boldsymbol{\Theta}'_b{}^T \mathbf{M}_{0 \rightarrow t}^T \mathbf{R}_t^{-1} (\mathbf{M}_{0 \rightarrow t} \boldsymbol{\Theta}'_b \mathbf{w} + M_{0 \rightarrow t}(\boldsymbol{\theta}, \mathbf{x}_0) - \mathbf{y}_k) \quad (19)$$

323 With this new formulation, we can further approximate

$$324 \quad \nabla \mathbf{J}(\mathbf{w}) = \mathbf{w} + \sum_{t=1}^K (\mathbf{M}_{0 \rightarrow t} \boldsymbol{\Theta}'_b)^T \mathbf{R}_t^{-1} (\mathbf{M}_{0 \rightarrow t} \boldsymbol{\Theta}'_b \mathbf{w} + M_{0 \rightarrow t}(\boldsymbol{\theta}, \mathbf{x}_0) - \mathbf{y}_k) \quad (20)$$

325 This formulation removes the need for the adjoint version of the model. An additional benefit of the 4DEnVar  
 326 method is that the gradient function value can be calculated for each ensemble member, since we are already  
 327 running an ensemble to approximate the prior error covariance matrix. This information, then, makes  
 328 straightforward determining the state estimate.

329 Compared to filter-based data assimilation methods (for example the Ensemble Kalman Filter; Evensen, 2003),  
 330 the variational methods do not estimate the posterior uncertainty directly. However, we used the method  
 331 established in Pinnington et al. (2021) to calculate the posterior distributions.

332 For the study here, we used the 4DEnVar algorithm provided in Quaife (2023). The gradient approach method  
 333 used there is BFGS2 (Saito and Nakano, 1997) from the GNU Scientific Library (GSL).

334 The 4DEnVar methodology holds crucial benefits for our model calibration even beyond the reduction in  
 335 computational cost compared to MCMC. Even though all the measurements used for calibration in this work are  
 336 from the same year, the model outputs are steady state products that take hundreds of simulated years to  
 337 produce. Hence, a 3-dimensional variational data assimilation (3DVar; Lorenc et al., 2000) cannot be applied  
 338 and the adjoint of the model would be required, as the gradient function needs to be calculated at the start of the  
 339 simulation. To complicate things further, the validity of the tangent-linear assumption would be questionable  
 340 due to the length of the simulation in this situation.

341

## 342 2.5 Calibration setup and uncertainty attribution

343 After having set up the algorithmic framework for both calibration methods for the selected LUCAS data points,  
 344 the first task was to complete twin experiments. In those, we randomly drew a value for each the parameter  
 345 chosen for calibration from the uncertainty distributions assigned for them in Table 1. Synthetic observations  
 346 were generated with the model using the new parameter set . Then, we performed the calibration with both  
 347 tested methods using these synthetic observations with their associated uncertainties set to be 1 % of those  
 348 synthetic observations and still using the same prior distribution established in Table 1. This allows us to check  
 349 if both methods were able to find the correct parameter sets in a situation where the true answer was known. For  
 350 the 4DEnVar, the additional importance of these tests is to assess the ensemble size dimension required to  
 351 consistently estimate the correct parameter set. This was accomplished by repeating the twin experiment  
 352 multiple times with different ensemble sizes and choosing the ensemble size where the calibration always found  
 353 the correct parameter set. The repetitions were necessary because the 4DEnVar ensemble members are  
 354 randomly drawn, therefore there are potential situations where a given ensemble size can retrieve the correct  
 355 parameter set several times in a row, but then fails on the next time.

356 After having set up the algorithmic framework for both calibration methods for the selected LUCAS data points,  
 357 the first task was to complete a twin experiment, where we generated synthetic observations from with the  
 358 model using a parameter set perturbed from the baseline parameters. Then, we performed the calibration with  
 359 these synthetic observations with their associated uncertainties set to be 1 % of those synthetic observations.  
 360 This allows us to check if both methods were able to find the correct parameter sets in a situation where the true

361 ~~answer was known. For the 4dEnVar, the additional importance of these tests is to assess the ensemble size~~  
362 ~~dimension required to consistently estimate the correct parameter set.~~

363 After the twin experiments have been conducted, the calibration itself is performed with the calibration dataset,  
364 before the validation runs are done for the validation dataset locations. In both situations the SOC is assumed to  
365 reflect a steady state. ~~It should be noted that with agricultural soils and commercial forests are expected to have~~  
366 ~~a large variability in litter input over a given time window, which does raise challenges for the steady state~~  
367 ~~approach. We are still including those data points in the analysis here as this is intended as a general calibration~~  
368 ~~across European ecosystems and there is no additional data to constrain those specific ecosystems, but this is~~  
369 ~~expected to be an additional uncertainty source. These runs were completed separately with two different  $f_{doc}$~~   
370 ~~values as a simple test regarding how NPP assumptions impact the MEMS model calibration.~~

371 As a part of the testing here, we also wished to experiment how varying assumptions regarding model drivers  
372 affected the potential differences between the calibration results. For our test case study on the impact of the  
373 NPP assumptions on the parameterization, we repeated the calibrations with a small adjustment. We changed the  
374  $f_{doc}$  value of grass- and croplands from 0.15 to 0.35. This increases the amount of the litter that is directly  
375 deposited to the soil and consequently adsorbed by the mineral matrix instead of being lost during the transition  
376 between the surface and soil carbon pools. ~~The logic behind this is that, in our expert opinion, it is likely that~~  
377 ~~there will be is at the higher proportion of exudates and root litter (i.e. low molecule weight compounds that can~~  
378 ~~directly sorbed by the soil minerals) inputted to entering the topsoil in grasslands and herbaceous crops to the~~  
379 ~~litter pools compared to forests. Thus, this change is suitable for a plausible change to the NPP assumptions and~~  
380 ~~makes an ideal test study to see how it affects the parameterization results and if the system depicted by the~~  
381 ~~parameterizations still remains consistent after the potential change.~~

382 When calculating the steady state, the MEMS model is simulated over the period of 700 years from an initial  
383 state vector (Supplemental Table 1). ~~of (0.35, 0.35, 0.15, 0., 0., 0.15, 0., 0., 3000., 0., 0.) for the MEMS C1 to~~  
384 ~~C9 pools, respectively. The values in pools C1, C2, C3 as well as C6 are used to ensure that there are no~~  
385 ~~numerical errors at the start of the simulation and do no impact the steady state at all. For the MAOM pool C9,~~  
386 ~~though, we initialised the model with some carbon already accumulated in order to reduce the number of~~  
387 ~~simulated years required for steady state.~~ Here, during calibration each LUCAS point is simulated for 700 years  
388 with the last output values compared to the measurements. At some sites, the MEMS model did not reach full  
389 steady state during this time, but the difference was within fractions of a percentage of the final steady state. As  
390 the change was so marginal already at this point, the shorter time period was chosen for computational  
391 efficiency.

392 As driver data at the European level, the model uses daily air temperature extracted from the E-OBS grid  
393 (Cornes et al., 2018). For each day of the year, an average temperature is calculated from a time series that spans  
394 from 2009-2018, with the temperature cycle then repeated for each year when calculating the steady state.  
395 Furthermore, the clay, sand and rock content of the soil as well as the soil bulk density and pH from LUCAS are  
396 used to determine soil properties driving SOC processes.

397 For Net Primary Production (NPP), first the average annual NPP over the decade 2000-2010 is extracted from  
398 the MODIS product MOD17A3 (Running et al., 2004) grid cell overlaying each LUCAS point. Then, a standard  
399 sine function is used to distribute the NPP across the year in order to produce the daily litter input. This  
400 approach was used instead of an averaged MODIS NPP annual time series as the NPP reflects the time when the  
401 atmospheric carbon is allocated into vegetation, not when the vegetation becomes litter input. Hence, we  
402 simplified the time series here, ~~although and, since the total annual NPP remains the same,~~ it is not expected to  
403 ~~meaningfully~~ affect the modelling results to a notable degree.

404 The total SOC measurement uncertainties from the LUCAS dataset are used as the uncertainties in this  
405 application. Since LUCAS protocol requires to take a composite soil sample (out of 5 samples), the uncertainty  
406 was estimated propagating the error associated to all variables for calculating SOC stock (i.e. SOC content,  
407 depth, rock fragment). We run a Monte Carlo simulation with 5000 draws, using a standard deviation derived  
408 from the coefficient of variation reported in Goidts et al., 2009 for the microsite scale, with a similar sampling  
409 scheme of LUCAS. It is important to note, though, that these values are calculated from mixed samples. Thus, it  
410 may be an underestimation of the real uncertainty for several reasons as, for example, how LUCAS samples are  
411 overall representative of the field conditions. However, we do not have more information concerning the SOC  
412 measurement uncertainties available.

413 Regarding the MAOM fraction, there is no established uncertainty estimate to utilize. Because of that, we  
414 assigned an uncertainty where the standard deviation was 5 percent of the measured MAOM value. This choice  
415 was driven by both a discussion with the data collection team about the reliability of the data and to ensure an  
416 appropriate weight during the calibration process. When the initial cost function is calculated using the baseline  
417 MEMS parameter set with this uncertainty, the total SOC values account for approximately two thirds of the  
418 cost function value, with the MAOM fraction being responsible for the remainder.

419 The prior uncertainty assigned to the parameters introduced challenges in this work. With MCMC, because we  
420 only use the prior parameter value range for the initial sampling, we were able to apply a uniform uncertainty  
421 distribution that was used to approximate the baseline parameter set ~~from~~ Robertson et al., 2019. For those  
422 parameters where the uncertainty was not provided, we approximated a wide enough uniform distribution  
423 around the assigned parameter value. The 4DEnVar method, though, requires a Gaussian uncertainty  
424 distribution as explained in section 2.4. As there is no prior information available, we used the baseline  
425 parameter values as the expected values, with the uncertainty represented by a standard deviation of 10 % of the  
426 parameter value. This uncertainty range, deliberately imposing a larger uncertainty, resulted in 4DEnVar  
427 calibration producing negative parameter values, which are naturally unrealistic. We will discuss the reasons  
428 and implications of this behaviour later.

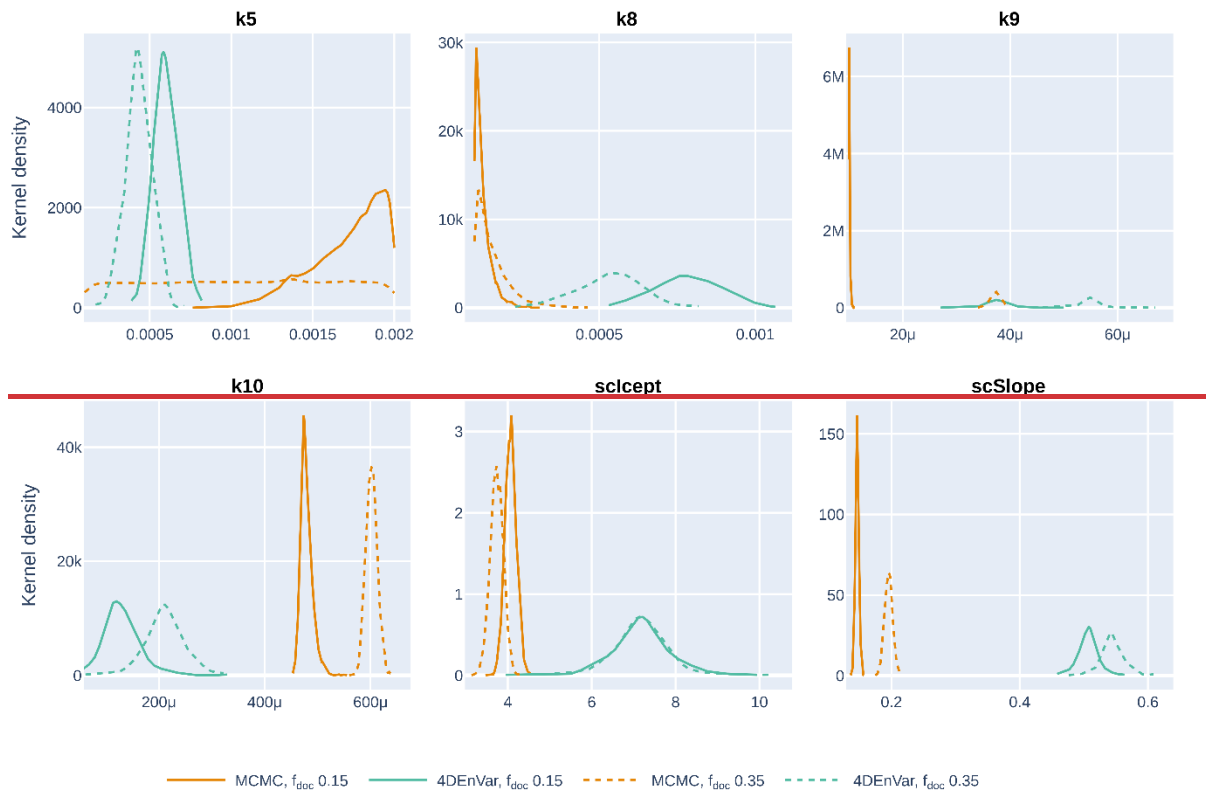
429 In some studies, for example, uncertainty has also been a parameter estimated with MCMC (Cailleret et al.,  
430 2020). Considering the meaningful unknowns regarding the uncertainty approximations, this would be a valid  
431 approach to be applied here. We did not estimate uncertainties for the initial MCMC/4DEnVar comparison, as  
432 varying the uncertainties might cause issues with the gradient approach methods and, consequently, would make  
433 it difficult to interpret the differences between the two. After the comparison, though, we did perform a MCMC  
434 calibration of MEMS, where we also estimated a scaling parameter for both total SOC and MAOM fraction  
435 uncertainties. However, these results are not shown here, as the calibration did not result in a successful  
436 convergence.

437

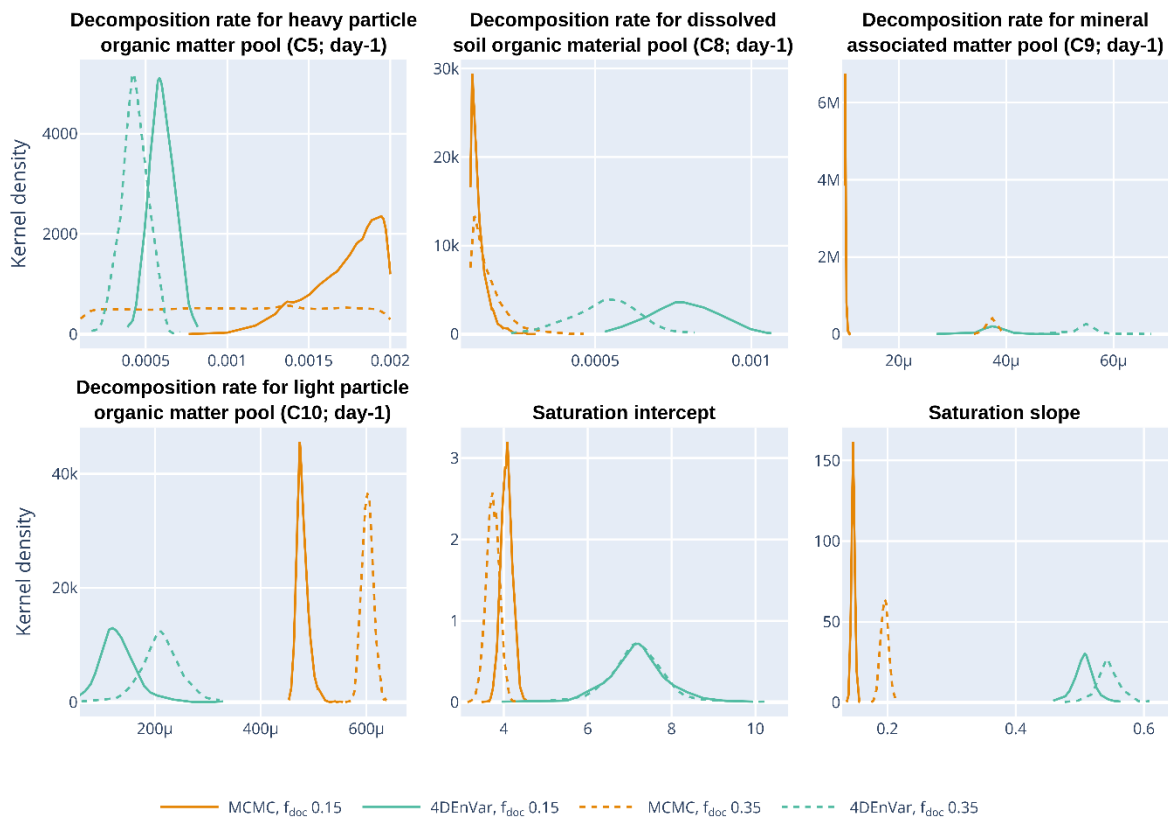
### 438 3 Results

439 The twin experiments (not shown) established that both methods were able to produce the true parameters when  
440 calibrating against synthetic observations. For 4DEnVar, the experiments established that an ensemble size of  
441 250 members consistently produced the parameters used to generate the synthetic observations for all repetitions  
442 of the twin experiment and, thus, we chose ~~to~~ this ensemble size for the 4DEnVar consequents.

443 The parameter distributions estimated by the MCMC and 4DEnVar calibration for both  $f_{doc}$  scenarios are  
444 presented in Figure 2. For clarity, the statistically likeliest parameter expected values from all the calibrations are  
445 in Table 3 and the standard deviations for the distributions in Supplemental Table 2. From these, we see that  
446 MCMC and 4DEnVar parameter sets differ ~~meaningfully~~ from each other ~~other~~ more than explained by their  
447 associated uncertainties in their value, but remain within the same range even when changing the NPP  
448 assumption. Furthermore, with the higher  $f_{doc}$  value, the uncertainty estimates with both methods end up being  
449 narrower, with the exception of  $k_5$  for the MCMC calibration parameter distributions produced by 4DEnVar  
450 remain approximately as wide even when they shift. Meanwhile with the MCMC calibration it produces wider  
451 distributions which represents larger uncertainties. It is also apparent that with three parameters ( $k_8$ ,  $k_9$  and  
452  $S_{c,slope}$ ), the MCMC produces expected values that are very close to the set boundaries when  $f_{doc}$  is set to 0.15  
453 while, when set to 0.35, those distributions are clearly within the given parameter ranges. This indicates that  
454 with the lower  $f_{doc}$ , the MCMC calibration struggles to find an acceptable parameter set within the accepted  
455 range. Similarly, the uncertainties with the 4DEnVar are quite wide, which implies that it also cannot effectively  
456 locate an ideal parameter set.



457



458

459 **Figure 2: Estimated parameter distributions for both MCMC (orange) and 4DnVar (green) calibrations with  $f_{doc}$**   
 460 **set to 0.15 (solid) and 0.35 (dashed). The  $\mu$  indicates a multiplier of  $10^{-6}$ .**

461 ~~The parameter distributions estimated by the MCMC and 4DEnVar calibration for both  $f_{doc}$  scenarios are~~  
 462 ~~presented in Figure 2. For clarity, the expected values from all the calibrations are in Table 3. From these, we~~  
 463 ~~see that MCMC and 4DEnVar parameter sets differ meaningfully from each other in their value, but remain~~  
 464 ~~within the same range even when changing the NPP assumption. Furthermore, with the higher  $f_{doc}$  value, the~~  
 465 ~~uncertainty estimates with both methods end up being narrower, with the exception of  $k_5$  for the MCMC~~  
 466 ~~calibration. It is also apparent that with three parameters ( $k_8$ ,  $k_9$  and  $SC_{slope}$ ), the MCMC produces expected~~  
 467 ~~values that are very close to the set boundaries when  $f_{doc}$  is set to 0.15 while, when set to 0.35, these~~  
 468 ~~distributions are clearly within the given parameter ranges. This indicates that with the lower  $f_{doc}$ , the MCMC~~  
 469 ~~calibration struggles to find an acceptable parameter set within the accepted range. Similarly, the uncertainties~~  
 470 ~~with the 4DEnVar are quite wide, which implies that it also cannot effectively locate an ideal parameter set.~~

471 The uncertainty distributions for 4DEnVar are generally wider than for MCMC in both cases. With 4DEnVar,  
 472 we repeated the calibration multiple times to ascertain that the randomness associated with the ensemble  
 473 selection did not result in meaningfully statistically different parameter sets. While there was variance in the  
 474 produced parameter sets, they overall remained within the uncertainty distribution for any single  
 475 estimation. While there was variance in the expected values, the standard deviation of the produced estimates  
 476 was smaller than the standard uncertainty projection for any single estimation.

477

	4DEnVar	MCMC
$k_5$	0.0006/0.00043	0.0019/0.0019
$k_8$	0.00078/0.00053	0.0001 /0.0001
$k_9$	0.000038/0.000055	0.00001/0.000037
$k_{10}$	0.00013/0.00021	0.00047/0.0006
$SC_{Icept}$	7.14/7.16	4.15/3.7
$SC_{Slope}$	0.51/0.54	0.144/0.197

478

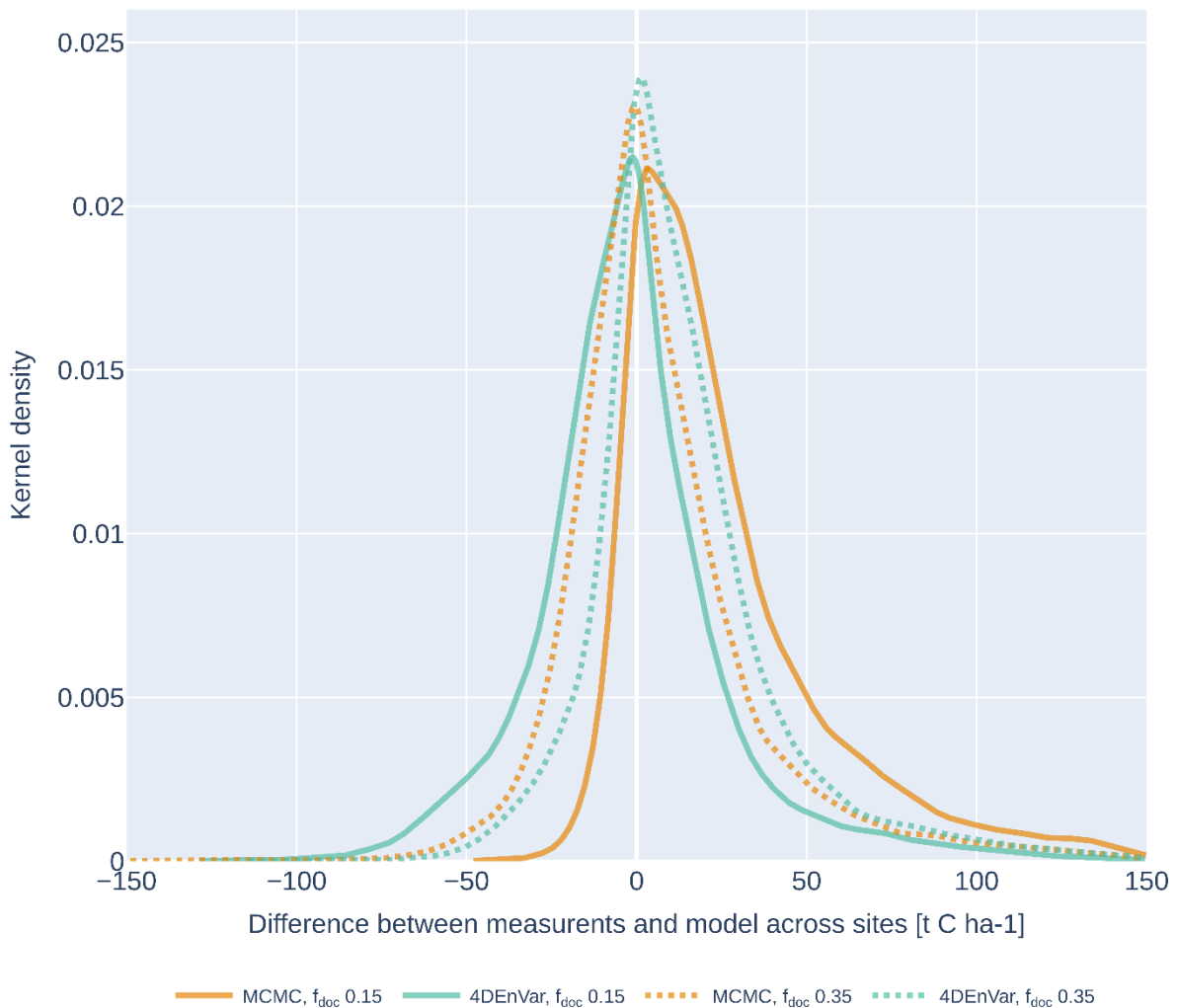
479 **Table 3: The expected statistically likeliest parameter values produced by the different calibration methods ~~and the~~**  
 480 **baseline parameters. The first value is for  $f_{doc}$  0.15, the second for  $f_{doc}$  0.35.**

481 To examine the impact of the new parameter sets, Figure 3 presents the differences between the measurements  
 482 and model projections across all the validation sites, while Table 4 shows both the Root Mean Square Error  
 483 (RMSE) and mean error (ME) representing bias in regard of the validation dataset for each parameter set. While  
 484 the 4DEnVar parameter sets produces a somewhat symmetric error distribution around zero in both calibrations,  
 485 with the high lower  $f_{doc}$  there is a slight slight apparent tendency towards negative positive errors. In contrast,  
 486 the MCMC error distribution shows a notable lean towards positive errors for the lower  $f_{doc}$ , which largely  
 487 disappears when the increasing direct litter input while with the higher  $f_{doc}$ , the bias is much reduced. Since the  
 488 SOC errors here are calculated as the measurement minus the model projection, this means that positive errors  
 489 reflect the parameter set systematically underestimating the SOC projections. It is notable that with the higher  
 490  $f_{doc}$ , the RMSE values for the two error distributions parameterizations are nearly identical very closer to each  
 491 other even with the larger positive bias of the 4DEnVar method.

492

	<u><math>f_{doc}</math> 0.15</u>	<u><math>f_{doc}</math> 0.35</u>
<u>MCMC</u>	<u>42.5 / 27.4</u>	<u>31.3 / 7.4</u>
<u>4DEnVar</u>	<u>29.8 / -1.9</u>	<u>32.0 / 14.2</u>

493 **Table 4: The error statistics for the different parameterizations with regard to the validation dataset. The**  
 494 **first value is for the root mean square error (RMSE) and the second for the mean error (ME). The unit**  
 495 **for all the values is t C ha<sup>-1</sup>.**

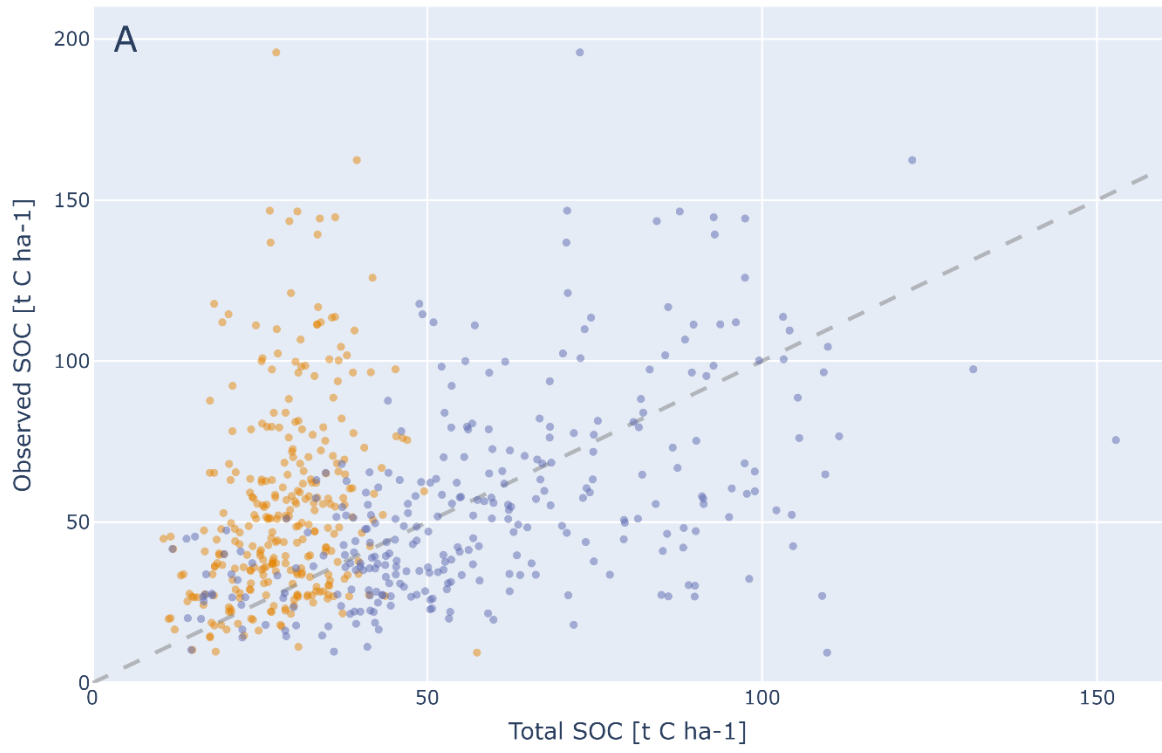


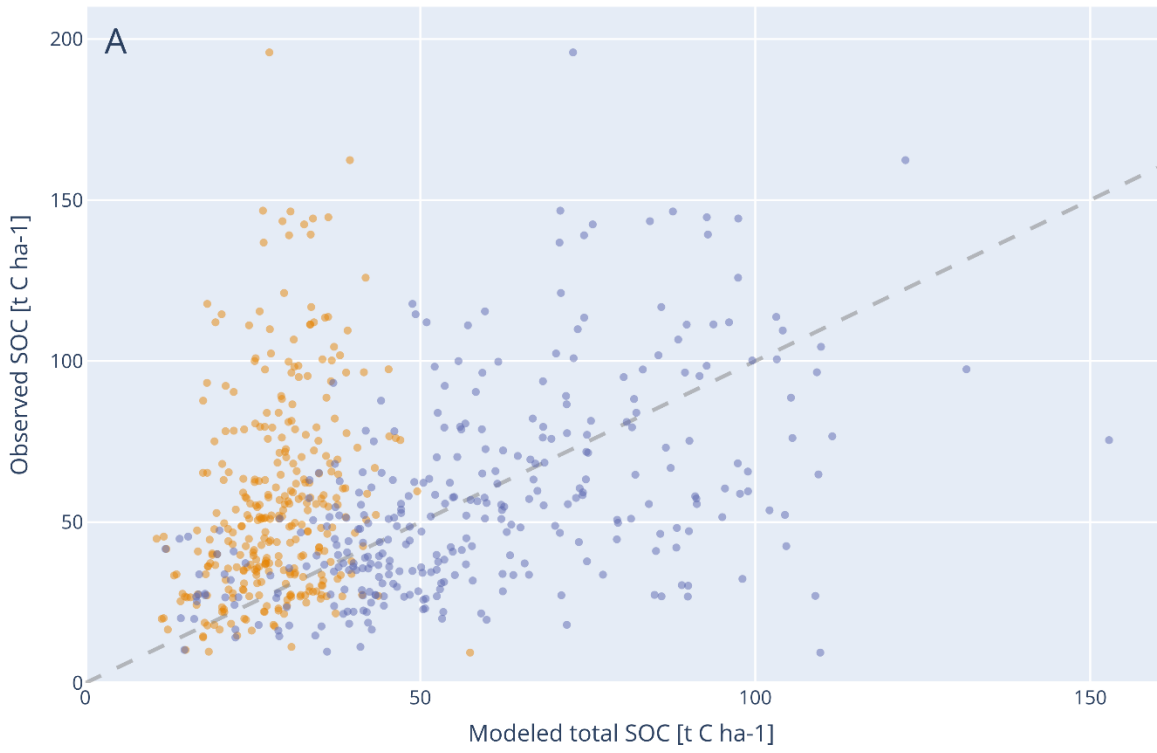
496

497 **Figure 3: The validation dataset error distributions for both MCMC (orange) and 4DnVar (green) calibrations with**  
 498  **$f_{doc}$  set to 0.15 (solid) and 0.35 (dashed).**

499 To better comprehend what is causing these systematic **MCMC errors** when  $f_{doc}$  is lower, we further examined  
 500 the actual calibration fit with both approaches in this scenario. Figure 4a shows how well the model SOC  
 501 projections follow the measurements and in Figure 4b the fit of the MAOM fraction with the 322 data points  
 502 used for calibration. From these comparisons, it is evident that, while the 4DnVar parameter set follows the  
 503 measurement trend more closely than the MCMC, the latter calibration in turn replicates the MAOM:SOC  
 504 fraction much better. We also note that there are also clear biases as the 4DnVar parameters constantly  
 505 underestimate the MAOM:SOC fraction, while there is a similar systemic underestimation of the total SOC with  
 506 the MCMC parameters. When comparing the calibration fits for the higher  $f_{doc}$  (**Not shown** [Supplementary](#)  
 507 [Figure XXX](#)), the behaviour remains similar with calibration methods, although the differences between the  
 508 measured and modelled values become smaller.

509 In further **When analysings** of the cost function ( $J$ ) for each estimated parameter set (**Not shown**), the MCMC  
 510 calibration resulted in a **meaningfully** lower  $J$  with the initial  $f_{doc}$  while, with the increased  $f_{doc}$  (i.e. from 0.15 to  
 511 0.35), the difference in  $J$  between the two approached **was much reduced** **becomes marginal**. However, when  
 512 further looking at both total SOC and MAOM fractions measurements in both cases, the 4DnVar produces a  
 513 better match with total SOC while, conversely, the MCMC parameter set results in a closer fit with the MAOM  
 514 fraction (MAOM: SOC) data. If we tighten the prior uncertainty used in the calibration, the 4DnVar produces a  
 515 different parameter set, though even those new parameters do still result in lower MAOM fractions in the  
 516 validation dataset projections.



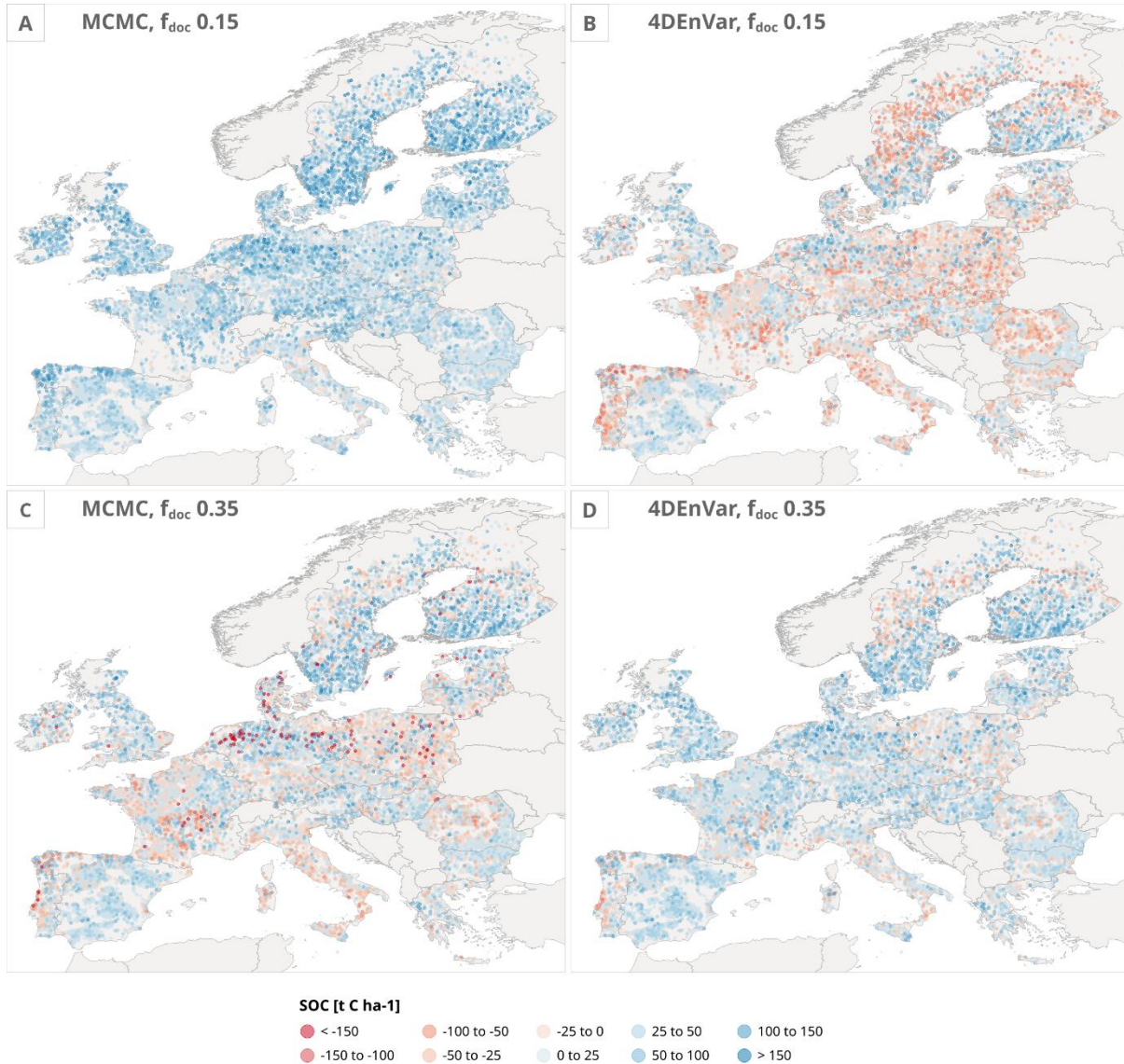


518

519 **Figure 4: For the calibration dataset, comparison between the modelled and measured a) Total SOC value and b)**  
 520 **MAOM:SOC fraction for both the MCMC and 4DenVar calibrations when  $f_{doc}$  was set to 0.15.**

521 Figure 5 shows the spatial distribution of the errors in Europe for both the MCMC and 4DEnVar parameter sets.  
 522 In the case of the lower  $f_{doc}$ , the MCMC underestimation is evident across Europe and, while the 4DEnVar map  
 523 is more evenly distributed, there are also clearly more local overestimations than when  $f_{doc}$  is set higher. In the  
 524 latter case, decrease in error can be seen across the whole Europe, with only a few clear areas, such as Nordic  
 525 countries and the Iberian Peninsula, with consistent bias in the error. However, what is intriguing is that across  
 526 central Europe, the prominent error points mirror each other. Where the MCMC parameter set produces  
 527 overestimations, the 4DEnVar parameter set conversely results in underestimations.

528



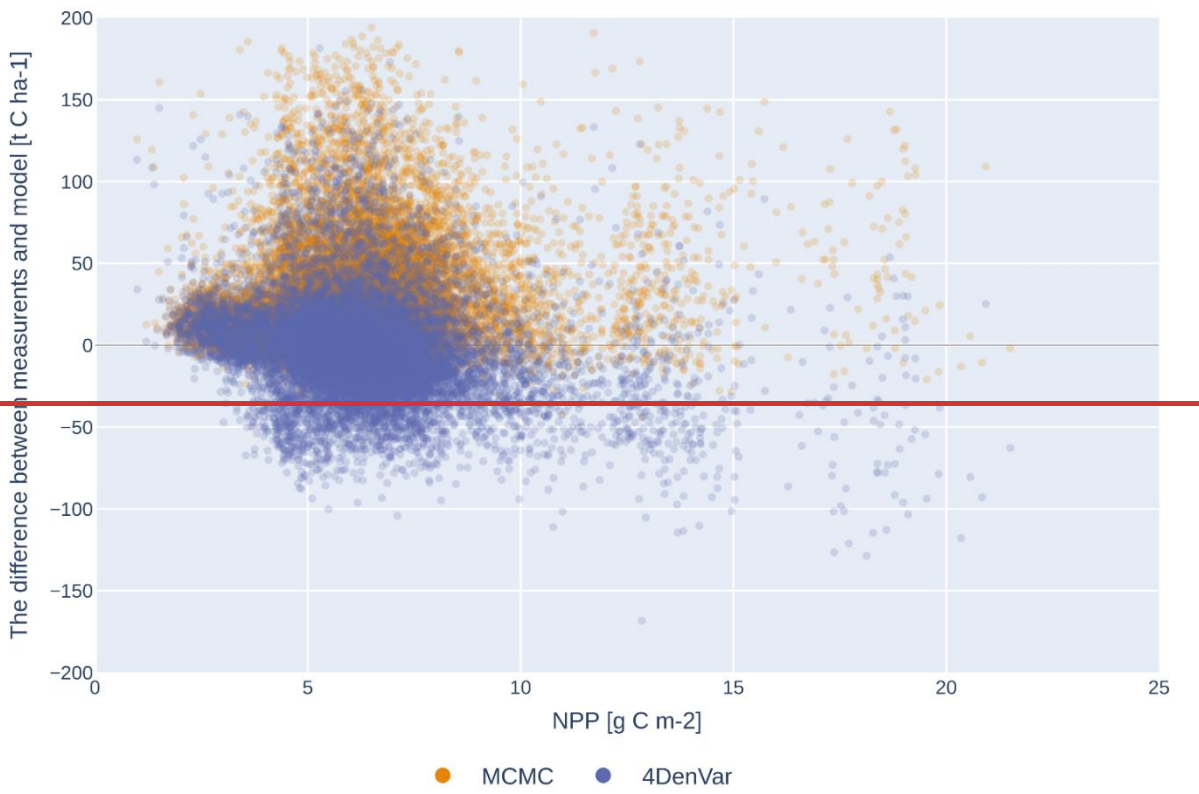
529

530

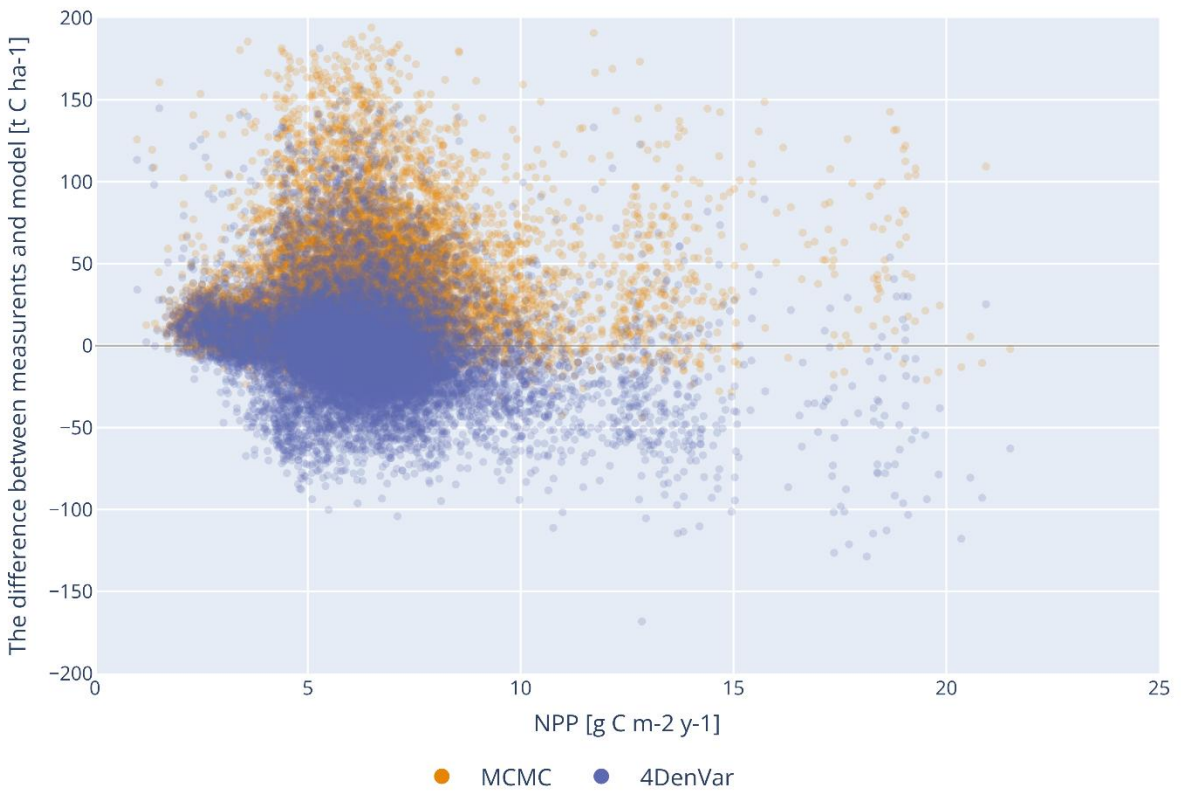
531 **Figure 5: Spatial error distributions across the LUCAS validation sites for a) MCMC with  $f_{doc}$  value of 0.15, b)**  
 532 **4DEnVar with  $f_{doc}$  value of 0.15, c) MCMC with  $f_{doc}$  value of 0.35, and d) 4DEnVar with  $f_{doc}$  value of 0.35**  
 533 **parameter sets**

534 Because of the pronounced errors when  $f_{doc}$  is set to the lower value, we further examined the relationship of  
 535 the SOC error with the NPP used as an approximation of the total litter input (Figure 6). During this  
 536 examination, it becomes evident that especially the MCMC parameter set projected a SOC underestimation  
 537 clustered around low NPP values. ~~When doing a further split into various ecosystems (Not shown), we see that~~  
 538 ~~the biases become much more pronounced with forest ecosystems.~~

539



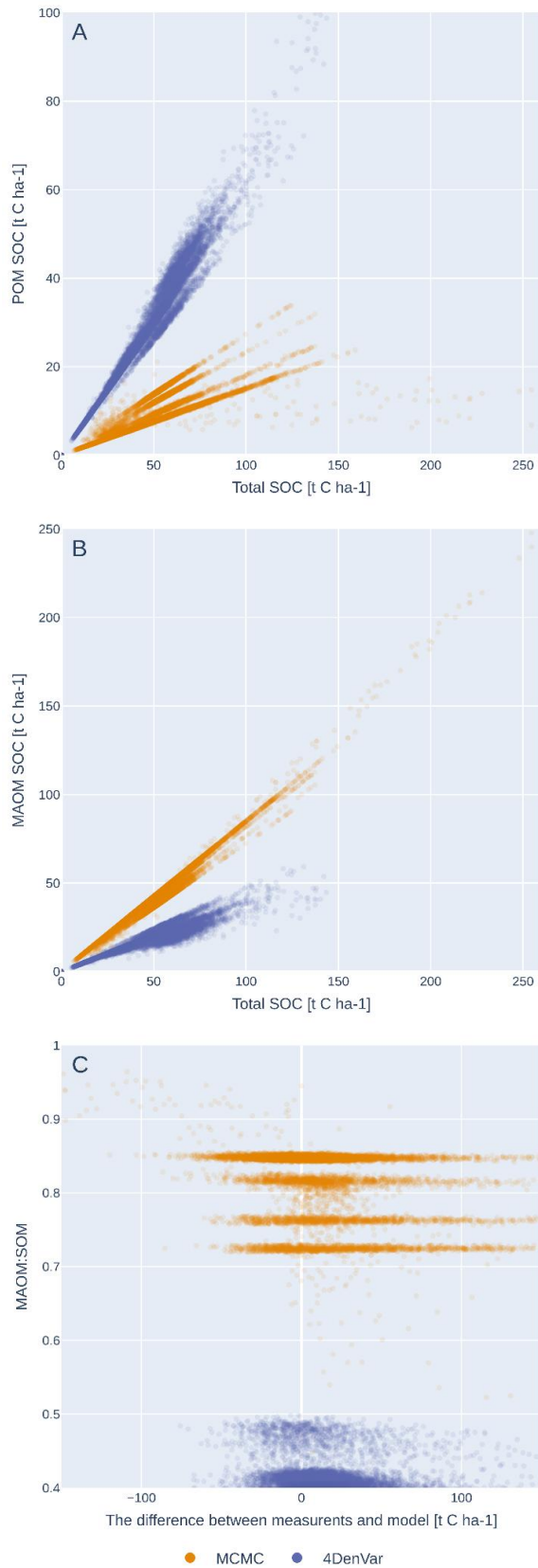
540



541

542 **Figure 6: Relationship between NPP and SOC projection error for both calibrated parameter sets after  $f_{doc}$  was set to**  
543 **0.15**

544 Finally, we examined the POM, MAOM and MAOM:SOC fractions in relation to the total projected SOC stock  
545 for the validation dataset with all calibrated parameter sets. Because of the systematic error when using the  
546 lower  $f_{doc}$  and, due to the general behaviour remaining similar between the two scenarios, we are only  
547 presenting the higher  $f_{doc}$  parameter set results here in Figure 7 for clarity. With the POM (Fig 7a) and MAOM  
548 (Fig 7b), we can see a similar differences between the two calibrations resulting from the initial calibrations.  
549 The MCMC parameterization still produces much higher MAOM stocks than 4DEnVar, and the latter  
550 parameterization contrastingly results in higher POM stocks. Additionally, POM with MCMC parameters  
551 remains at lower values than with the 4DEnVar parameters while, for the 4DEnVar parameters, MAOM hits a  
552 ceiling sooner than for the MCMC parameters. To further examine the impact of these behaviours on the  
553 projections, Figure 7c illustrates the relationship between the MAOM fraction and model error across all the  
554 validation data points. Analysing the results further, we found that the very high SOC projections with both  
555 MCMC and baseline parameters occurred in specific circumstances, where both NPP and annual temperatures  
556 were low (not shown), and hence we attribute this to a structural issue within the model that arises in specific  
557 conditions rather than the parameterization per se.



558

559 **Figure 7: The model projected a) POM, b) MAOM stocks in relation to the total modelled SOC stocks as well as c)**  
 560 **The MAOM:SOM ratio in relation to the model error across the LUCAS sites after  $f_{doc}$  was increased from 0.15 to**  
 561 **0.35.**

562

## 563 4 Discussion

### 564 4.1 Comparison between the performances of MCMC and 4DEnVar calibration methods

565 As seen in the results, the 4DEnVar approach is a straightforward tool for calibrating the MEMS v1 model with  
566 LUCAS data, as valid as the MCMC approach. Both had issues with the first parameterization attempt when it  
567 came to the validation dataset, but performed similarly when the direct litter fraction to soil was increased.  
568 Hence, the central problem with the first calibration attempt was not due to the calibration method itself. This  
569 supports 4DEnVar as a meaningful approach for initial calibration of soil carbon models, especially considering  
570 the massive difference in the required computational costs. For MCMC, the 100 000 iterations used here took  
571 over a month to compute on our HPC server while, simulating the 250 ensemble members without using  
572 parallelization, took approximately four hours. It should be noted that the MCMC calibration did begin to  
573 converge to the final values already after 40 000 iterations, but there is a risk in accepting the first-stable  
574 parameter-set/local cost function minima after such a relatively short calibration cycle. The computational cost  
575 for calibration from having to spin-up to steady state is a known issue with land system models in general  
576 (Raoult et al., 2025).

577 What is striking, though, is that-how much the parameter sets produced by the two calibration methods in both  
578 litter distribution scenarios differ from each ~~to a meaningful extent~~, even with the higher  $f_{doc}$ , they when they  
579 perform approximately equally well with regard to the total SOC measurements in the the-validation dataset. As  
580 mentioned in the Introduction, equifinality, a situation where there exists multiple parameter sets that produce  
581 similar model outputs, is a known issue in ecosystem modelling and is evidently represented by the results here.  
582 The notable element here is that the calibration method itself determines the resulting parameter set as even  
583 when repeated, the MCMC calibration approach does not suggest the solution is in the same part of the  
584 parameter space as the 4DEnVar results indicate. Generally, twin experiments are efficient first pass to test for  
585 equifinality and the challenge can be addressed by reducing the amount of parameters being calibrated, but here  
586 there are questions how much those efforts can be relied on in assessing equifinality. In further analysis of the  
587 cost function ( $J$ ) for each estimated parameter set, the MCMC calibration resulted in a meaningfully lower  $J$   
588 with the initial  $f_{doc}$  while, with the increased  $f_{doc}$  (i.e. from 0.15 to 0.35), the difference in  $J$  between the two  
589 approached becomes marginal. However, when further looking at both total SOC and MAOM fractions  
590 measurements in both cases, the 4DEnVar produces a better match with total SOC while, conversely, the  
591 MCMC parameter set results in a closer fit with the MAOM fraction (MAOM: SOC) data. If we tighten the  
592 prior uncertainty used in the calibration, the 4DEnVar produces a different parameter set, though even those  
593 new parameters do still result in lower MAOM fractions in the validation dataset projections.

594 While we are not certain of what is driving these systematic differences between calibration sets, we  
595 hypothesize that one crucial component is that the total SOC and MAOM fraction measurements appear to  
596 incentivize contradicting model behaviours. Our twin experiment results support this theory as, with synthetic  
597 datasets, we were able to retrieve the same parameter set of both total SOC and MAOM that internally coherent  
598 with the model dynamics. This tension is especially evident when the  $f_{doc}$  is lower and there is less litter to  
599 distribute between the SOC pools. In that situation, MCMC is still able to find a solution by forcing a reduction  
600 in the decomposition rate for the MAOM pool and increasing the decomposition rate for the POM pool. This  
601 leads to a high MAOM fraction but at the cost of lower POM pool values and, consequently, a tendency to  
602 project lower SOC values. Meanwhile, this conflict between the two measurement types does seem to cause  
603 issues with the gradient approach method applied by 4DEnVar to determine the ideal parameter set. This could  
604 be because the disagreement between the data sources will create such a degree of noise in the likelihood space  
605 that determining a correct gradient descent from a collection of ensembles will become much more challenging.  
606 Simultaneously, though, this vulnerability in the 4DEnVar could be exploited in future work to quickly test if  
607 different measurement types and drivers are compatible within the model framework.

608 These results further highlight the fundamental impact of the priors on the calibration results, especially with the  
609 4DEnVar approach, that has been recognized as a larger challenge in ecosystem modelling (Dietze, 2017).  
610 While experimenting with the initial setup, we found that the 4dEnVar calibration produced unrealistic  
611 parameter values with negative decomposition rates, if prior was set to be too loose. This remained true even  
612 when increasing the  $f_{doc}$  value, although then the uncertainty could be loosened slightly more. Our hypothesis is  
613 that, while the MCMC iterative approach allows setting boundaries for the region where the values are sampled,  
614 such hard constraints are not present with the 4DEnVar. Additionally, the 4DEnVar does rely on the first order  
615 Taylor expansion, making it vulnerable to non-linear behaviours. Thus, incongruities resulting from missing

616 model processes such as soil moisture, for example, can drive the parameterization beyond acceptable values if  
617 there is not a sufficient prior constrain implemented. This could be a partial explanation for the Iberian  
618 Peninsula error biases visible in Fig 5 as the soil moisture dynamics are much more complicated in arid climates  
619 vulnerable to drought (Almendra-Martin et al., 2021). A further limitation is that the 4DEnVar algorithm used  
620 here draws the ensemble members by sampling the prior distribution. While this is a logical approach when  
621 those distributions are reliably approximated, here we do not know what the prior distributions are and must use  
622 a tight uncertainty range in order to avoid unrealistic estimations. Consequently, our application of 4DEnVar  
623 samples the parameter space in a more limited manner than would be preferable.

624 The lack of knowledge on prior distributions for the parameters is an obstacle that is further hindered by the lack  
625 of reliable measurement uncertainty estimates. An important aspect of Bayesian statistics is that the weight of an  
626 individual information source depends on how accurate it is in comparison to the other available information  
627 sources. Hence, the width of the prior uncertainty that we can assign to constrain the parameter estimate to  
628 remain in a reasonable range is dependent on the measurement uncertainty. In this work, those uncertainties  
629 were so low that we had to use a relatively narrow prior parameter range for the 4DEnVar approach.  
630 Furthermore, as detailed in the Methods section, we do not have reliable approximations of the measured  
631 MAOC:SOC fraction uncertainties. Their uncertainty here is, thus, defined by how much weight we wished to  
632 give them in relation to the total SOC measurements. When we tested a larger measurement error, which in turn  
633 allowed us to increase the prior parameter distribution for the 4DEnVar without producing unrealistic estimates,  
634 the 4DEnVar ensembles also changed with the new values moving farther away from the baseline values. The  
635 implication is that the 4DEnVar is much more sensitive to the measurement uncertainty representation than  
636 MCMC, due to how the prior constraint is applied.

637 Naturally this underlines the overall importance of providing reliable measurement uncertainties along with  
638 measurements themselves, but that is not something a model user can simply produce by themselves. When  
639 implementing the calibration, based on the results here we would recommend of initially looking through the  
640 calibration data and confirming that all the values there are sensible for the model/system being calibrated. As a  
641 more practical solution, it is possible to repeat the 4DEnVar calibration multiple times by using the previous  
642 posterior distributions as the priors to the next cycle. This way it is possible to ensure that the resulting  
643 parameter set is not simply because the prior had been set too far from the correct value and thus partially  
644 reduce the impact of the assigned prior distribution. However, the downside of repeating the calibration cycle in  
645 this manner is that not only does it reduce the impact of the prior, but each iteration reduces the resulting  
646 uncertainty distribution. Thus, the final parameter distributions would be artificially too confident. While the  
647 repeated calibration is a worthwhile tool in certain circumstances, it always needs to be implemented with great  
648 care and consideration.

649

#### 650 **4.2 The impact of the NPP assumption on the calibrated parameter set performance**

651 Our results clearly underline how the fundamental assumptions regarding the NPP, as a litter proxy, impact the  
652 model calibration results. The lower  $f_{doc}$  resulted in a noticeable bias on total SOC predictions, especially with  
653 regard to the MCMC calibration. Another encouraging aspect of the work is that the differences between the  
654 two calibration methods results remain consistent even when changing the litter input assumption. This supports  
655 the capability of using the quicker 4DEnVar calibration to explore the impact of the NPP assumptions on the  
656 parameterization as any signal noted there should be reflected also in MCMC results.

657 What complicates future work is that coefficients associated with litter input are challenging to calibrate  
658 simultaneously with parameters associated with SOC decomposition, as their influence on the SOC overlap too  
659 much. It is important to note that while the focus in this experimentation has been the  $f_{doc}$  value, what it actually  
660 represents is the assumption of dividing NPP between upper- and below ground biomass as it reflects the  
661 amount of litter deposited directly into the soil. This is a central assumption that has to be included in some  
662 manner in SOC modelling and is represented by the plant species traits assigned to the surface vegetation. This  
663 highlights why better understanding of the vegetation qualities of the ecosystem being modelled is important for  
664 calibrating even simple SOC models.

665 In addition, eAs for even attempting to calibrate the NPP/litter coefficients simultaneously would first  
666 necessitate determining which exact coefficients would be calibrated. For example, in our case, there is first the

667 question how well the MODIS NPP product represents reality for different systems. Then, part of that NPP is  
668 removed to represent economic activity before it is distributed to the four MEMS initial pools based on the three  
669 coefficients. Any of these three parts can be altered to change the final NPP input to the soil in different ways,  
670 but there is really no certainty at the moment what is the correct manner to better regulate the NPP based litter  
671 input. This complicated relationship in the surface vegetation driving litterfall and the SOC state has been shown  
672 in prior work such as in Raczka et al. (2021). There when they used remote sensing data to constrain their model  
673 state, while this improved their modelled aboveground biomass and carbon exchange accuracy, it also caused  
674 their modelled SOC accuracy to decrease because they were only using the aboveground data for both systems.

675 Adding to the challenges discussed above is that the various assumptions are not expected to be spatially  
676 homogeneous even in the same ecosystem type. For instance, the Nordic countries, especially Sweden and  
677 Finland, are dominated by economic forests where the NPP-to-litter pathway is heavily impacted by the growth  
678 stage as newly growing forest will have a large NPP, but not a corresponding amount of litter due to mortality.  
679 This could be connected to bias seen in the northern Europe in Fig 5. Another example would be agricultural  
680 ecosystems as climate conditions affect which crops will be dominant in a given region. The type of crops  
681 naturally affects its traits as, for instance, the root depth distribution, which in turn is expected to impact the soil  
682 carbon stocks (Fan et al., 2016). These various components could be a reason why when analysing global soil  
683 databases, there is a weak statistical relationship between NPP and SOC despite that dynamic being well  
684 understood (Luo et al., 2021).

685 Naturally this is not to questioning the use of NPP as a litter input for soil carbon models. Rather it is another  
686 reminder on how important it is to be aware of the various assumptions related to the NPP and remain consistent  
687 with them while running the calibrated model in various systems. Additionally, when doing future SOC  
688 projections, the uncertainties related to the various NPP/litter assumptions should be considered during analysis.

689 The error distributions for both calibration methods when applying the higher litter input is in itself worthy of  
690 analysis. The MEMSv1 model used is lacking several dynamics that are known to impact soil carbon stock, such  
691 as soil moisture (Falloon et al., 2011), various nutrient cycles (Gardenas, et al., 2011; Feng et al., 2023) and  
692 mycorrhiza abundance (Hawkins et al., 2023). However, when considering the multitude of simplifications  
693 made to calculate the steady state approximations using parameters calibrated with data from 322 sites, the error  
694 distribution for the 17 000+ validation sites is remarkably-much narrower than we initially expected. Which  
695 raises question how much of a further performance issue could be expected with addition of new processes?  
696 And, consequently, how can this limited data be used to evaluate which processes are most important for future  
697 projections?

698 Notably, while the spatial presentation of the model error under the higher  $f_{doc}$  shows only few regions where the  
699 differences between the two model errors are consistently larger than 10 tons of carbon per hectare, such as the  
700 Nordic countries, the MAOM fraction projections by the two model calibrations differ systematically to a  
701 meaningful degree. For instance, 4DEnVar calibration resulted in a higher turnover rate of the MAOM pool,  
702 which in turn causes lower MAOM stocks. Both calibration methods are adjusting the parameters to produce  
703 lower total SOC, as the baseline parameters tend to overestimate the SOC stocks, but they solve the issue with  
704 very different representations of the internal SOC state that would have a major impact on future projections.  
705 With the current available information, it is not possible to evaluate which of the two states is more realistic;  
706 while the MCMC modelled MAOM fractions are on average high for all ecosystems (Georgiou et al., 2022), the  
707 LUCAS dataset leans towards arable soils where the MAOM fraction is expected to be larger in the top layer  
708 than for forests (Schrumpf et al, 2013; Sokol et al, 2022).

709 These outcomes emphasise the importance of carefully considering how model performance improvements are  
710 assessed with large-scale datasets such as the LUCAS measurement data, since the total SOC seems not  
711 sufficient which is in line with previous studies (Braakhekke et al., 2014; Guo et al., 2022). This is especially  
712 relevant as the model validation should be a crucial aspect of model choice regarding different SOC  
713 sequestration projects (Garsia et al., 2023). New measurement analysis methods allow for more efficient  
714 POM/MAOM fractioning of SOC samples (Delahaie et al., 2023), thus providing more detailed measurements  
715 to use during validation. However, as our results show, the SOC fractions might not be compatible with the total  
716 SOC measurements within the model context and indicate that there are missing processes within our model  
717 framework. Consequently, their value might be rather to evaluate what missing processes are needed within the  
718 model than validate existing parameterizations. Another approach for evaluation could be to examine the model  
719 performance within sub-regions or individual ecosystems instead of weighing it against the total dataset at once.

720 A more nuanced approach to do this would be to use a hierarchical Bayesian approach (Gelman and Hill, 2007),  
721 but that requires more research on the applicability of that approach in solving the challenges highlighted by our  
722 results.

723

## 724 5 Conclusions

725 Calibrating soil organic carbon (SOC) models with large scale data sets is always a challenge due to the  
726 computational cost involved. Furthermore, numerous assumptions are made regarding model drivers that can  
727 potentially deeply affect the parameterization. In our work presented in this article, we have shown that  
728 4DnVar parameterization produces ~~as good validation performance~~the approximately same RMSE for the  
729 validation dataset as the traditional and more cumbersome MCMC DEzs algorithm when the soil litter input is  
730 increased and actually outperforms in this metric the MCMC with the lower litter input. However, the parameter  
731 sets produced by the calibration methods ~~meaningfully~~ differed from each other as did the model states they  
732 projected. Even though the total SOC<sub>s</sub> were similar, the difference between shorter lived POM and longer lived  
733 MAOM compounds was large enough to notably impact future projections. We also conducted a simple  
734 experiment to assess the impact of ~~a slight change in~~ how the soil litter input ~~was calculated~~is distributed  
735 among different litter pools. ~~From those results, we did see that this change did result in meaningfully different~~  
736 ~~parameterizations, but also that the comparisons between the two methods remained similar~~. These results  
737 showed that while the litter input adjustment did impact the calibration, the general model behaviour produced  
738 by the two calibration methods remained similar. This implies, if it holds true with further testing, that the  
739 differences between the behaviours of the two calibration methods are not dependent on the driver data. Another  
740 facet of these results is that it confirms how large of an impact ecosystem related assumptions have on the  
741 resulting calibrations. The work here highlights how further consideration is required how to evaluate the model  
742 performances, especially on a larger scale. However, they also establish the fast 4DnVar as a valid exploration  
743 tool that allows testing various scenarios with much more ease than the traditional MCMC approach. This will  
744 make it more pragmatically possible to assess how various assumptions impact ecosystem model results as well  
745 as better include those uncertainties in future projections as the various drivers are altered by climate change.

746

### 747 Data/Code availability

748 The MEMS v1 model version, the calibration algorithms as well as all the data used for calibration and  
749 validation is available on Zenodo at <https://doi.org/10.5281/zenodo.17314989> (Viskari et al. (2025)).

750

### 751 Author contributions

752 TV is the primary author of the manuscript and was responsible for creating the calibration framework as well  
753 as analysing the results. TQ provided expert assistance in implementing the 4DnVar and insight into the  
754 results. FF helped setting up the environmental driver data and created the graphical presentation of the results.  
755 YZ is one of the creators the MEMS v1 model and offered expertise on prior calibration approaches with the  
756 model. EL is PI of the project that this research is a part of and was responsible for the LUCAS dataset model  
757 efforts.

758

### 759 Competing interests:

760 The authors declare that they have no conflict of interests.

761

### 762 Acknowledgments

763 This research was supported by the Carbon Removal on Land project, an administrative arrangement (n. 36662)  
764 between the Directorate-General Climate (DG-CLIMA) and the Joint Research Centre of the European

765 Commission. Tristan Quaife was funded under the International Programme of the UKRI National Centre for  
766 Earth Observation (NE/X006328/1).

767 References:

- 768 [Almendra-Martin, L., Martinez-Fernandez, J., Gonzalez-Zamora, A., Benito-Verdugo, and Herrero-Jimenez,](#)  
769 [C.M.: Agricultural Drought Trends on the Iberian Peninsula: An Analysis Using Modeled and Reanalysis Soil](#)  
770 [Moisture Products. \*Atmosphere\*, 12\(2\), 236, 10.3390/atmos12020236, 2021](#)
- 771 Abramoff, R.Z., Guenet, B., Zhang, H., Georgiou, K., Xu, X., Viscarra Rossel, R.A., Yuan, W., And Ciais, P.:  
772 Improved global-scale predictions of soil carbon stocks with Millennial Version 2. *Soil Biol Biochem*, **164**,  
773 108466, 2022
- 774 Bellassen, V., Stephan, N., Afriat, M., Alberola, E., Barker, A., Chang, J.-P., Chiquet, C., Cochran, I., Deheza,  
775 M., Dimopoulos, C., Foucherot, C., Jacquier, G., Morel, R., Robinson, R., and Shishlov, I.: Monitoring,  
776 reporting and verifying emissions in the climate economy. *Nature Climate Change*, **5(4)**, 319-328, 2015
- 777 [Beylat, S., Raoult, N., Bacour, C., Douglas, N., Quaipe, T., Bastrikov, V., Rayner, P.J., and Peylin, P.: Towards](#)  
778 [the assimilation of atmospheric CO<sub>2</sub> concentration data in a land surface model using adjoint-free variational](#)  
779 [methods. \*Geosci Model Dev\*, 18, 7501-7527, 10.5194/gmd-18-7501-2025, 2025](#)
- 780 [Braakhekke, M.C., Beer, C., Schrumf, M., Ekici, A., Ahrens, B., Hoosbeek, M.R., Kruijff, B., Kabat, P., and](#)  
781 [Reichstein, M.: The use of radiocarbon to constrain current and future soil organic matter turnover and transport](#)  
782 [in a temperate forest. \*J Geophys Res Biogeosciences\*, 119\(3\), 372-391, 10.1002/2013JG002420, 2014](#)
- 783 [Brunmayer, A.S., Hagedorn, F., Moreno Duborgel, M., Minich, L.I., and Graven H.D.: Radiocarbon analysis](#)  
784 [reveals underestimation of soil organic carbon persistence in new-generation soil model. \*Geosci Model Dev\*, 17,](#)  
785 [5961-5985, 2024](#)
- 786 Buttner, G: "CORINE land cover and land cover change products." In *Land use and land cover mapping in*  
787 *Europe: practices & trends* (pp. 55-74). Dordrecht: Springer Netherlands
- 788 Cailleret, M., Bircher, N., Hartif, F., Hulsmann, L., and Bugmann, H.: Bayesian calibration of a growth-  
789 dependent tree mortality model to simulate the dynamics of European temperate forests. *Ecol Appl*, **30**, e02021,  
790 10.1002/eap.2021, 2020
- 791 [Cambardella, C.A., and Elliot, E.T.: Particulate Soil Organic Matter Changes across a Grassland Cultivation](#)  
792 [Sequence. \*Soil Sci Soc Am J\*, 56\(3\), 777-783, 1992](#)
- 793 Campbell, E.E., Parton, W.J., Soong, J.L., Paustian, K., Hobbs, N.T., and Cotrufo, M.F.: Using litter chemistry  
794 controls on microbial processes on partition litter carbon fluxes with Litter Decomposition and Leaching  
795 (LIDEL) model. *Soil Biol Biochem*, **100**, 160-174, 2016
- 796 Cao, J., Li, Y., Biswas, A., Holden, N.M., Adamowski, J.F., Wang, F., Hong, S., and Qin, Y.: Grassland  
797 biomass allocation across continents and grazing practices and its response to climate and altitude. *Agric For*  
798 *Met*, 356, 110176, 10.1016/j.agrformet.2024.110176, 2024
- 799 Coleman, K., and Jenkinson, D. S.: RothC-26.3-A Model for the turnover of carbon in soil. In *Evaluation of soil*  
800 *organic matter models: Using existing long-term datasets* (pp. 237-246). Berlin, Heidelberg: Springer Berlin  
801 Heidelberg, 1996
- 802 Cornes, R.C., Van Der Schrier, G., Van Den Besselaar, E.J., and Jones, P.D.: An ensemble version of the E-  
803 OBS temperature and precipitation data sets. *J Geophys Res*, **123(17)**, 9391-9409, 2018
- 804 Cornwell, W. K., Cornelissen, J. H. C., Amatangelo, K., Dorrepaal, E., Eviner, V. T., Godoy, O., Hobbie, S. E.,  
805 Hoorens, B., Kurokawa, H., Perez-Harguindeguy, N., Quested, H. M., Santiago, L. S., Wardle, D. A., Wright, I.  
806 J., Aerts, R., Allison, S. D., van Bodegom, P., Brovkin, V., Chatain, A., Callaghan, T. V., Diaz, S., Garnier, E.,  
807 Gurvich, D. E., Kazakou, E., Klein, J. A., Read, J., Reich, P. B., Soudzilovskaia, N. A., Vaieretti, M. V., and  
808 Westoby, M.: Plant species traits are the predominant control on litter decomposition rates within biomes  
809 worldwide, *Ecol. Lett.*, **11**, 1065–1071, 2008.
- 810 Cotrufo, M.F., Ranalli, M.G., Haddix, M.L., Six, J., and Lugato, E.: Soil carbon storage informed by particulate  
811 and mineral-associated organic matter. *Nat Geosci*, **12**, 989-994, 2019

- 812 Delahaie, A.A., Barre, P., Baudin, F., Arrouays, D., Bispo, A., Boulonne, L., Chenu, C., Jolivet, C., Martin,  
813 M.P., Ratie, C., Saby, N.P.A., Savignac, F., and Cecillon, L.: Elemental stoichiometry and Rock-Eval® thermal  
814 stability of organic matter in French topsoils. *Soil*, 9, 209-229, 10.5194/soil-9-209-2023, 2023
- 815 ~~Delahaie, A.A., Cecillon, L., Stojanova, M., Abiven, S., Arbelet, P., Arrouays, D., Baudin, F., Bispo, A.,  
816 Boulonne, L., Chenu, C., Heinonsalo, J., Jolivet, C., Karhu, K., Martin, M., Pacini, L., Poeplau, C., Ratie, C.,  
817 Roudier, P., Saby, N.P.A., Savignac, F., and Barre, P.: Investigating the complementarity of thermal and  
818 physical soil organic carbon fractions. *Soil*, **10(2)**, 795-812, 2024~~
- 819 Dietze, M.: Ecological forecasting. Princeton University Press. [10.1515/9781400885459](https://doi.org/10.1515/9781400885459), 2017
- 820 Douglas, N., Quaife, T., and Bannister, R.: Exploring a hybrid ensemble–variational data assimilation technique  
821 (4DEnVar) with a simple ecosystem carbon model. *Environmental Model Softw*, 106361, 2025
- 822 Evensen, G.: The ensemble Kalman filter: Theoretical formulation and practical implementation. *Ocean dyn*, **53**,  
823 343-367, 2003
- 824 Falloon, P., Jones, C.D., Ades, M., and Paul, K.: Direct soil moisture controls of future global soil carbon  
825 changes: An important source of uncertainty. *Glob Biochem Cycles*, **25(3)**, 10.1029/2010GB003938, 2011
- 826 ~~Fan, J., McConkey, B., Wang, H., and Janzen, H.: Root distribution by depth for temperate agricultural crops.  
827 *Field Crops Res*, **189**, 68-74, 10.1016/j.fcr.2016.02.013, 2016~~
- 828 Feng, J., Song, Y., and Zhu, B.: Ecosystem-dependent responses of soil carbon storage to phosphorus  
829 enrichment. *New Phytol*, **238(6)**, 2363-2374, 10.1111/nph.18907, 2023
- 830 Gardenas, A.I., Agren, G.I., Bird, J.A., Clarholm, M., Hallin, S., Ineson, P., Katterer, T., Knicker, H., Nilsson,  
831 S.I., Nasholm, T., Ogle, S., Paustian, K., Persson, T., and Stendahl, J.: Knowledge gaps in soil carbon and  
832 nitrogen interactions – From molecular to global scale. *Soil Biol Biochem*, **43(4)**, 702-717,  
833 10.1016/j.soilbio.2010.04.006, 2011
- 834 Garsia, A., Moinet, A., Vazquez, C., Creamer, R.E., and Moinet, G.Y.K.: The challenge of selecting an  
835 appropriate soil organic carbon simulation model: A comprehensive global review and validation assessment.  
836 *Glob Change Biol*, 29(20), 5760-5774, 10.1111/gcb.16896, 2023
- 837 Gelman, A. and Hill, J.: Data analysis using regression and multilevel/hierarchical models. Cambridge  
838 University Press, Cambridge, 2007
- 839 Georgiou, K., Jackson, R.B., Vinduskova, O., Abramoff, R.Z., Ahlstrom, A., Feng, W., Harden, J.W.,  
840 Pellegrini, A.F.A., Polley, H.W., Soong, J.L., Riley, W.J., and Torn, M.S.: Global stocks and capacity of  
841 mineral-associated soil organic carbon. *Nat Commun*, **13**, 3797, 2022
- 842 Geyer, C.J.: Practical Markov Chain Monte Carlo. *Stat Sci*, **7(4)**, 473-483, 1992
- 843 Goidts, E., van Wesemael, B., and Crucifix, M.: Magnitude and sources of uncertainties in soil organic carbon  
844 (SOC) stock assessment at various scales. *Eur J Soil Sci*, **60**, 723-739, 10.1111/j.1365-2389.2009.01157.x, 2009
- 845 ~~Guo, X., Viscarra Rossel, R.A., Want, G., Xiao, L., Wang, M., Zhang, S., and Luo Z.: Particulate and mineral-  
846 associated organic carbon turnover revealed by their long-term dynamics. *Soil Biol Biochem*, **173**, 108780,  
847 10.1016/j.soilbio.2022.108780, 2022~~
- 848 Gurung, R.B., Ogle, S.M., Breidt, F.J., Williams, S.A., and Parton, W.J.: Bayesian calibration of the DayCent  
849 ecosystem model to simulate soil organic carbon dynamics and reduce model uncertainty. *Geoderma*, **376**,  
850 114529, 10.1016/j.geoderma.2020.114529, 2020
- 851 Hartig, F., Minunno, F., Paul, S., Cameron, D., Ott, T., and Pichler, M.: BayesianTools: General-Purpose  
852 MCMC and SMC Samples and Tools for Bayesian Statistics. R package version 0.1.8, [https://CRAN.R-](https://CRAN.R-project.org/package=BayesianTools)  
853 [project.org/package=BayesianTools](https://CRAN.R-project.org/package=BayesianTools) (last access: 2 May 2025), 2019.
- 854 Harmon, M. E., Moreno, A., and Domingo, J. B.: Effects of partial harvest on the carbon stores in Douglas-  
855 fir/western hemlock forests: a simulation study. *Ecosystems*, **12**, 777-791, 2009

- 856 Hawkins, H.-J., Cargill, R.I.M., Van Nuland, M.E., Hagen, S.C., Field, K.J., Sheldrake, M., Soudzilovskaia,  
857 N.A., and Kiers, E.T.: Mycorrhizal mycelium as a global carbon pool. *Current Biology*, **33(11)**, R560-R573,  
858 2023
- 859 Heuvelink, G.B.M., Angelini, M.E., Poggio, L., Bai, Z., Batjes, N.H., van den Bosch, R., Bossio, D., Estella, S.,  
860 Lehmann, J., Olmedo, G.F., and Sanderman, J.: Machine learning in space and time for modelling soil organic  
861 carbon change. *Eur J Soil Sci*, **72(4)**, 1607-1623, 2021
- 862 Huang, X.-Y., Xiao, Q., Barker, D.M., Zhang, X., Michalakes, J., Huang, W., Henderson, T., Bray, J., Chen, Y.,  
863 Ma, Z., Dudhia, J., Guo, Y., Zhang, X., Won, D.-J., Lin, H.-C., and Kuo, Y.-H.: Four-dimensional Variational  
864 Data Assimilation for WRF: Formulation and Preliminary Results. *Mon Weather Rev*, 137(1), 299-314,  
865 [10.1175/2008MWR2577.1](https://doi.org/10.1175/2008MWR2577.1), 2009
- 866 Jevon, F.V., Polussa, A., Lang, A.K., Munger, J.W., Wood, S.A., Wieder, W.R., and Bradford, M.A.: Patterns  
867 and controls of aboveground litter inputs to temperate forests. *Biogeochemistry*, **161**, 335-352, 2022
- 868 Lavallee, J.M., Soong, J.L., and Cotrufo, M.F.: Conceptualizing soil organic matter into particulate and mineral-  
869 associated forms to address global change in the 21<sup>st</sup> century. *Glob Change Biol*, **26(1)**, 261-273,  
870 [10.1111/gcb.14859](https://doi.org/10.1111/gcb.14859), 2020
- 871 Le Dimet, F., and Talagrand, O.: Variational algorithms for analysis and assimilation of meteorological  
872 observations: Theoretic aspects. *Tellus*, **38A**, 97-110, 1986
- 873 [Leuthold, S.J., Haddix, M.L., Lavallee, J., and Cotrufo, M.F.: Physical fractioning techniques. Encyclopedia of](#)  
874 [Soils in the Environment, 2, 68-80, 10.1016/B978-0-12-822974-3.00067-7, 2023](#)
- 875 Liu, C., Xiao, Q. and Wang, B.: An Ensemble-Based Four-Dimensional Variational Data Assimilation Scheme.  
876 Part I: Technical Formulation and Preliminary Test. *Mon Weather Rev*, **136(9)**, 3363-3373,  
877 [10.1175/2008MWR2312.1](https://doi.org/10.1175/2008MWR2312.1), 2008
- 878 Lorenc, A.C., Ballard, S.P., Bell, R.S., Ingleby, N.B., Andrews, P.L.F., Barker, D.M., Bray, J.R., Clayton, A.M.,  
879 Dalby, T., Li, D., Payne, T.J., and Saunders, F.W.: The Met Office global three-dimensional variational data  
880 assimilation scheme. *Quarterly J Royal Meteorol Soc*, **126(570)**, 2991-3012, 2000
- 881 Loria, N., Lai, R., and Chandra, R.: Handheld In Situ Methods for Soil Organic Carbon Assessment.  
882 *Sustainability*, **16(13)**, 5592, 2024
- 883 Lugato, E., Lavallee, J.M., Haddix, M.L., Panaganos, P., and Cotrufo, M.F.: Different climate sensitivity of  
884 particulate and mineral-associated soil organic matter. *Nature Geoscience*, **14(5)**, 295-300, 2021
- 885 [Luo, Z., Viscarra-Rossel, R.A., and Qian, T.: Similar importance of edaphic and climate factors for controlling](#)  
886 [soil organic carbon stocks of the world. Biogeosciences, 18\(6\), 10.5194/bg-18-2063-2021, 2021](#)
- 887 [Marschmann, G.L., Pagel, H., Kugler, P., and Streck, T.: Equifinality, sloppiness, and emergent structures of](#)  
888 [mechanistic soil biochemical models. Environ Model Softw, 122, 104518, 10.1016/j.envsoft.2019.104518, 2019](#)
- 889 Mathers, C., Black, C.K., Segal, B.D., Gurung, R.B, Zhang, Y., Easter, M.J., Williams, S., Motew, M.,  
890 Campbell, E.E., Brummit, C.D., Paustian, K., and Kumar, A.A.: Validating DayCent-CR for cropland soil  
891 carbon offset reporting at a national scale. *Geoderma*, **438**, 116647, [10.1016/j.geoderma.2023.116647](https://doi.org/10.1016/j.geoderma.2023.116647), 2023
- 892 Matthews, E.: Global litter production, pools, and turnover times: Estimates from measurement data and  
893 regression models. *J Geophys Res Atmos*, **102(D15)**, 18771-18800, 1997
- 894 Nemo, Klumpp, K., Coleman, K., Dondini, M., Goulding, K., Hasting, A., Jones, M.B., Leifeld, J., Osborne, B.,  
895 Saunders, M., Scott, T., Teh, Y.A., and Smith, P.: Soil Organic Carbon (SOC) Equilibrium and Model  
896 Initialisation Methods: an Application to the Rothamsted Carbon (RothC) Model. *Environ Model Assess*, **22**,  
897 215-229, 2017
- 898 Orgiazzi, A., Ballabio, C., Panagos, P., Jones, A., and Fernande-Ugalde, O.: LUCAS soil, the largest expandable  
899 soil dataset for Europe: a review. *Eur J Soil Sci*, **69**, 140-153, 2018

900 Papaioannou, I., Betz, W., Zwirgmaier, K., and Straub, D.: MCMC algorithms for subset  
901 simulation. *Probabilistic Eng Mech*, *41*, 89-103, 2015

902 Peylin, P., Bacour, C., MacBean, N., Leonard, S., Rayner, P., Kuppel, S., Koffi, E., Kane, A., Maignan, F.,  
903 Chevallier, F., Ciais, P., and Prunet, P.: A new stepwise carbon cycle data assimilation system using multiple  
904 data streams to constrain the simulated land surface carbon cycle. *Geosci Model Dev*, *9*, 3321-3346,  
905 10.5194/gmd-9-3321-2016, 2016

906 Pierson, D., Lohse, K.A., Wieder, W.R., Patton, N.R., Facer, J., de Graaff, M.-A., Georgiou, K., Seyfried, M.S.,  
907 Flerchinger, G., and Will, R.: Optimizing process-based models to predict current and future soil organic carbon  
908 stocks at high-resolution. *Sci Rep*, *12*, 10824, 2022

909 Pinnington, E.M., Casella, E., Dance, S.L., Lawless, A.S., Morison, J.I., Nichols, N.K., Wilkinson, M. and  
910 Quaife, T.L.: Investigating the role of prior and observation error correlations in improving a model forecast of  
911 forest carbon balance using Four-dimensional Variational data assimilation. *Agric For Meteorol*, *228*, 299-314,  
912 2016

913 Pinnington, E., Quaife, T., Lawless, A., Williams, K., Arkebauer, T., and Scoby, D.: The Land Variational  
914 Ensemble Data Assimilation Framework: LAVENDAR v1.0.0. *Geosci Model Dev*, *13*, 55-69, 10.5194/gmd-13-  
915 55-2020, 2020

916 Pinnington, E., Amezcua, J., Cooper, E., Dadson, S., Ellis, R., Peng, J., Robinson, E., Morrison, R., Osborne, S.,  
917 and Quaife, T.: Improving soil moisture prediction of a high-resolution land surface model by parameterising  
918 pedotransfer function through assimilation of SMAP satellite data. *Hydrol Earth Sys Sci*, *25(3)*, 1617-1641,  
919 10.5194/hess-25-1617-2021, 2021

920 Quaife, T.: C implementation of 4DEnVar using the GSL. Github repository,  
921 [https://github.com/tquaife/4DEnVar\\_engine](https://github.com/tquaife/4DEnVar_engine), 2023

922 Raczka, B., Hoar, T.J., Duarte, H.F., Fox, A.M., Anderson, J.L., Bowling, D.R., and Lin, J.C.: Improving  
923 CLM5.0 Biomass and Carbon Exchange Across the Western United States Using a Data Assimilation System. *J*  
924 *Adv Model Earth Sys*, e2020MS002421, [10.1029/2020MS002421](https://doi.org/10.1029/2020MS002421), 2021

925 Raoult, N.M., Jupp, T.E, Cox, P.M., and Luke, C.M.: Land-surface parameter optimisation using data  
926 assimilation techniques: the adJULES system v1.0. *Geosci Model Dev*, *9*, 2833-2852, 10.5194/gmd-9-2833-  
927 2016, 2016

928 Raoult, N., Douglas, N., MacBean, N., Kolassa, J., Quaife, T., Roberts, A.G., et al.: Parameter estimation in land  
929 surface models: Challenges and opportunities with data assimilation and machine learning. *J Adv Model Earth*  
930 *Sys*, *17*, e2024MS004733, [10.1029/2024MS004733](https://doi.org/10.1029/2024MS004733), 2025

931 Robertson, A.D., Paustian, K., Ogle, S., Wallenstein, M.D., Lugato, E., and Cotrufo, M.F.: Unifying soil organic  
932 matter formation and persistence frameworks: the MEMS model. *Biogeosciences*, *16*, 1225-1248, 10.5194/bg-  
933 16-1225-2019, 2019

934 Roy, V.: Convergence diagnostics for markov chain monte carlo. *Annu Rev Stat Appl*, *7(1)*, 387-412, 2020

935 Ruder, S.: An overview of gradient descent optimization algorithms. *arXiv preprint arXiv:1609.04747*, 2016

936 Rumpel, C., Amiraslani, F., Chenu, C., Cardenas, M.G., Kaonga, M., Koutika, L.-S., Ladha, J., Madari, B.,  
937 Shirato, Y., Smith, P., Soudi, B., Soussana, J.-F., Whitehead, D., and Wollenberg, E.: The 4p1000 initiative:  
938 opportunities, limitations and challenges for implementing soil organic carbon sequestration as a sustainable  
939 development strategy. *Ambio*, *49(1)*, 350-360, 10.1007/s13280-019-01165-2, 2020

940 Running, S.W., Nemani, R.R., Heinsch, F.A., Zhao, M., Reeves, M., and Hashimoto, H.: A continuous satellite-  
941 derived measure of global terrestrial production. *BioScience*, *54*, 547-560, 2004

942 Saito, K., and Nakano, R.: Partial BFGS update and efficient step-length calculation for three-layer neural  
943 network. *Neural computation*, *9(1)*, 123-141, 1997

944 Scharlemann, J.P.W., Tanner, E.V.J., Hiederer, R., and Kapos, V.: Global soil carbon: understanding the largest  
945 terrestrial carbon pool. *Carbon Manag*, **5**, 81-91, [doi.org/10.4155/cmt.13.77](https://doi.org/10.4155/cmt.13.77), 2014

946 Schlamadinger, B., Bird, N., Johns, T., Brown, S., Canadell, J., Ciccacese, L., Dutschke, M., Fiedler, J.,  
947 Fischlin, A., Fearnside, P., Corner, F., Freibauer, A., Frumhoff, P., Hoehne, N., Kirschbaum, M.U.F., Labat, A.,  
948 Marland, G., Michaelowa, A., Montanarella, L., Moutinho, P., Murdiyarso, D., Pena, N., Pingoud, K.,  
949 Rakonczay, Z., Rametsteiner, E., Rock, J., Sanz, M.J., Schneider, U.A., Shvidenko, A., Skutsch, M., Smith, P.,  
950 Somogyi, Z., Trines, E., Ward, M., and Yamagata, Y.: A synopsis of land use, land-use change and forestry  
951 (LULUCF) under the Kyoto Protocol and Marrakech Accords. *Environ Sci Policy*, **10(4)**, 271-282, 2007

952 Schrumpf, M., Kaiser, K., Guggenberger, G., Persson, T., Kogel-Knabner, I., and Schulze, E.-D.: Storage and  
953 stability of organic carbon in soils as related to depth, occlusion with aggregates, and attachment to minerals.  
954 *Biogeosciences*, **10**, 1675-1691, 10.5194/bg-10-1675-2013, 2013

955 [Sierra, C.A., Malghani, S., and Muller, M.: Model structure and parameter identification of soil organic matter  
956 models. \*Soil Biol Biochem\*, \*\*90\*\*, 197-203, 10.1016/j.soilbio.2015.08.012, 2015](https://doi.org/10.1016/j.soilbio.2015.08.012)

957 Smith, P., Soussana, J.-F., Angers, D., Schipper, L., Chenu, C., Rasse, D.P., Batjes, N.H., van Egmond, F.,  
958 McNeill, S., Kuhnert, M., Arias-Navarro, C., Olesen, J.E., Chirinda, N., Fornara, D., Wollenberg, E., Alvaro-  
959 Fuentes, J., Sanz-Cobena, A., and Klumpp, K.: How to measure, report and verify soil carbon change to realize  
960 the potential of soil carbon sequestration for atmospheric greenhouse gas removal. *Glob Change Biol*, **26(1)**,  
961 219-241, 2020

962 Sokol, N.W., Whalen, E.D., Jilling, A., Kallenbach, C., Pett-Ridge, J., and Georgiou, K.: Global distribution,  
963 formation and fate of mineral-associated soil organic matter under changing climate: A trait-based perspective.  
964 *Funct Ecol*, **36(6)**, 1411-1429, 10.1111/1365-2435.14040, 2022

965 ter Braak, C.J.F., and Vrugt, J.A.: Differential evolution Markov chain with snooker updater and fewer chains.  
966 *Stat Comput*, **18**, 435e446, 10.1007/s11222-008-9104-9, 2008

967 Thepaut, J.N., and Courtier, P.: Four-dimensional variational data assimilation using the adjoint of a multilevel  
968 primitive-equation model. *Quarterly J Royal Meteorol Soc*, **117(502)**, 1225-1254, 1991

969 Tippett, M.K., Anderson, J.L., Bishop, C.K., Hamill, T.M.,

970 Tuomi, M., Thum, T., Jarvinen, H., Fronzek, S., Berg, B., Harmon, M., Trofymow, J.A., Sevanto, S., and Liski,  
971 J.: Leaf litter decomposition – Estimates of global variability based on the Yasso07 model. *Ecol Modell*, **220**,  
972 3362-3371, 10.1016/j.ecolmodel.2009.05.016, 2009

973 van den Berg, N.J., van Soest, H.L., Hof, A.F., den Elzen, M.G.J., van Vuuren, D.P., Chen, W., Drouet, L.,  
974 Emmerling, J., Fujimori, S., Hoehne, N., Koberle, A.C., McCollum, D., Schaeffer, R., Shekhar, S.,  
975 Vishwanathan, S.S., Vrontisi, Z., and Blok, K.: Implications of various effort-sharing approaches for national  
976 carbon budgets and emission pathways. *Clim Change*, **162**, 1805-1822, 2020

977 Viskari, T., Pusa, J., Fer, I., Repo, A., Vira, J., and Liski, J.: Calibrating the soil organic carbon model Yasso20  
978 with multiple datasets. *Geosci Model Dev*, **15(4)**, 1735-1752, 10.5194/gmd-15-1735-2022, 2022

979 Viskari, T., Quaipe, F., Fahl, F., Zhang, Y., and Lugato, E.: Comparing the MEMS v1 model performance with  
980 MCMC and 4DEnVar calibration methods over a continental soil inventory,  
981 <https://doi.org/10.5281/zenodo.17314989>, (Last accessed October 10 2025), 2025

982 Vrugt, J.A.: Markov chain Monte Carlo simulation using theDream software package: Theory, concepts, and  
983 MATLAB implementation. *Environ Model Softw*, **75**, 273-316, 10.1016/j.envsoft.2015.08.013, 2016

984 Wieder, W. R., Grandy, A. S., Kallenbach, C. M., and Bonan, G. B.: Integrating microbial physiology and  
985 physio-chemical principles in soils with the Microbial-Mineral Carbon Stabilization (MIMICS)  
986 model. *Biogeosciences*, **11(14)**, 3899-3917, 2014

987 Yu, W., Huang, W., Weintraub-Leff, S.R., and Hall, S.J.: Where and why do particulate organic matter (POM)  
988 and mineral-associated organic matter (MAOM) differ among diverse soils? *Soil Biol Biochem*, **172**, 108756,  
989 2022